the plant journal

SEB Society for Experimental Biology

The Plant Journal (2019) doi: 10.1111/tpj.14275

Genetic buffering of cyclic AMP in *Arabidopsis thaliana* compromises the plant immune response triggered by an avirulent strain of *Pseudomonas syringae* pv. *tomato*

Wilma Sabetta[1,†,‡], Elodie Vandelle[2,†], Vittoria Locato[3,†], Alex Costa[4,†], Sara Cimini[3], Andrea Bittencourt Moura[2,§], Laura Luoni[4], Alexander Graf[5], Luigi Viggiano[6], Laura De Gara[3], Diana Bellin[2], Emanuela Blanco[1,*] and Maria C. de Pinto[6,*]

[1]*Institute of Biosciences and Bioresources, CNR, Research Division Bari, Via Amendola 165/A, 70126 Bari, Italy,*
[2]*Department of Biotechnology, University of Verona, Strada Le Grazie 15, 37134 Verona, Italy,*
[3]*Unit of Food Science and Human Nutrition, University Camps Bio-Medico of Rome, via Alvaro del Portillo, 21, 00128 Rome, Italy*
[4]*Department of Biosciences, University of Milan, Via G. Celoria 26, 20133 Milano, Italy*
[5]*Max Planck Institute of Molecular Plant Physiology, Potsdam-Golm, Germany and*
[6]*Department of Biology, University of Bari "Aldo Moro", Via Orabona 4, 70125 Bari, Italy*

Received 26 July 2018; revised 23 December 2018; accepted 24 January 2019.
*For correspondence (e-mails emanuela.blanco@ibbr.cnr.it; mariaconcetta.depinto@uniba.it).
†These authors contributed equally to this work.
‡Present address: Spin Off Sinagri S.r.l., University of Bari "Aldo Moro" Via Amendola 165/A, Bari, Italy.
§Present address: Departamento de Fitossanidade, Universidade Federal de Pelotas, Rua Gomes Carneiro 1, 96010-970, Pelotas RS, Brazil.

SUMMARY

Cyclic AMP plays important roles in different physiological processes, including plant defence responses. However, as little information is known on plant enzymes responsible for cAMP production/degradation, studies of cAMP functions have relied, to date, on non-specific pharmacological approaches. We therefore developed a more reliable approach, producing transgenic *Arabidopsis thaliana* lines overexpressing the 'cAMP-sponge' (cAS), a genetic tool that specifically buffers cAMP levels. In response to an avirulent strain of *Pseudomonas syringae* pv. *tomato* (*PstAvrB*), cAS plants showed a higher bacterial growth and a reduced hypersensitive cell death in comparison with wild-type (WT) plants. The low cAMP availability after pathogen infection delayed cytosolic calcium elevation, as well as hydrogen peroxide increase and induction of redox systems. The proteomic analysis, performed 24 h post-infection, indicated that a core of 49 proteins was modulated in both genotypes, while 16 and 42 proteins were uniquely modulated in WT and cAS lines, respectively. The involvement of these proteins in the impairment of defence response in cAS plants is discussed in this paper. Moreover, *in silico* analysis revealed that the promoter regions of the genes coding for proteins uniquely accumulating in WT plants shared the CGCG motif, a target of the calcium-calmodulin-binding transcription factor AtSR1 (*Arabidopsis thaliana* signal responsive1). Therefore, following pathogen perception, the low free cAMP content, altering timing and levels of defence signals, and likely acting in part through the mis-regulation of AtSR1 activity, affected the speed and strength of the immune response.

Keywords: cAMP, hypersensitive response, cytosolic calcium, hydrogen peroxide, redox systems, proteomic pattern, *Arabidopsis thaliana*, *Pseudomonas syringae*.

INTRODUCTION

Environmental factors such as biotic and abiotic stresses can affect plant growth, development and productivity. As a consequence of a generally disturbed cell homeostasis, a prompt response to alleviate the impact of stress is necessary. Major players of this early phase of defence response are signalling molecules, including secondary messengers such as calcium ions (Ca^{2+}) or cyclic nucleotides (cNMP; Gao *et al.*, 2012; Van Damme *et al.*, 2014; Hussain *et al.*, 2016).

In higher plants, the presence and the biological role of 3′,5′-cyclic adenosine monophosphate (cAMP) have been, for a long time, a matter of debate. This situation is firstly

due to its low cellular concentration (typically between 40 and 170 pmol g^{-1} fresh weight (FW)) and secondly to the technical difficulties related to its detection (Gehring, 2010; Gehring and Turek, 2017). Moreover, plant adenylyl-cyclases (AC) and cAMP phosphodiesterases (PDE), responsible for cAMP synthesis and catabolism, respectively, have not been isolated and/or fully characterized, although evidence of their activity has been reported (Gehring and Turek, 2017; Bianchet *et al.*, 2019).

Advances in molecular studies and analytical methods for the detection, imaging and quantification of cNMPs have allowed definition of a more precise role for cAMP in plant growth and defence responses. Several studies have reported that cAMP has direct and/or indirect roles in many developmental plant processes, spanning from cell cycle (Ehsan *et al.*, 1998; Sabetta *et al.*, 2016) and pollen tube growth (Moutinho *et al.*, 2001) to stomata closure (Curvetto *et al.*, 1994; Newton and Smith, 2004) and ion homeostasis (Anderson *et al.*, 1992; Bolwell, 1995; Trewavas, 1997). More recently, through a proteomic approach, the involvement of cAMP-mediated signalling has been reported in response to temperature and light stresses, and in the regulation of photosynthesis and photorespiration (Thomas *et al.*, 2013; Donaldson *et al.*, 2016).

Intracellular levels of cAMP have been shown to also increase during plant immune response (Bolwell, 1992; Kurosaki and Nishi, 1993; Cooke *et al.*, 1994; Zhao *et al.*, 2004; Jiang *et al.*, 2005; Ma *et al.*, 2009; Lu *et al.*, 2016). The plant immune response is initiated upon the recognition of pathogen-associated molecular patterns (PAMPs) by pattern recognition receptors (PRRs), localized at the plasma membrane, resulting in the induction of a basal defence response known as PAMP-triggered immunity (PTI; Jones and Dangl, 2006). Plants have also evolved a second layer of defence that involves receptor encoded by resistance genes to detect pathogen-derived effectors. This second level of active resistance is called effector-triggered immunity (ETI) and leads to a stronger and more massive immune response, called hypersensitive response (HR), which culminates with a programmed cell death localized at the site of infection (Jones and Dangl, 2006; Cui *et al.*, 2015). Pharmacological studies, including treatments with cell-permeating cAMP analogues and mammalian stimulators/inhibitors of AC, have been pursued to unravel cAMP function in both PTI and ETI. The quick increment of intracellular cAMP level in response to AC activators, forskolin, theophylline or cholera toxin, in carrot cell cultures, stimulates the production of 6-methoxymellein, an antifungal phytoalexin, and mediates the activation of Ca^{2+} uptake (Kurosaki *et al.*, 1987; Kurosaki and Nishi, 1993). *Medicago sativa* seedlings challenged with an elicitor derived from a phytopathogenic fungus or treated with a permeable cAMP analogue display a stimulation of phenylalanine ammonia lyase activity and the synthesis of the phytoalexin medicarpin (Cooke *et al.*, 1994). Another recent example is the stimulation of the phenylpropanoid pathway in Arabidopsis seedlings upon the exogenous application of cAMP derivatives (Pietrowska-Borek and Nuc, 2013).

Studies carried out on elicited french bean and Arabidopsis cell cultures have also shown the dependence of hydrogen peroxide (H_2O_2) generation on cAMP, Ca^{2+} and K^+ fluxes (Bolwell *et al.*, 1999, 2002; Bindschedler *et al.*, 2001; Davies *et al.*, 2006). As an immediate consequence of cAMP-dependent signalling transduction, Ca^{2+} and K^+ fluxes are generally affected throughout the targeting of membrane cyclic nucleotide-gated channels (CNGCs) (Assmann, 1995; Ma *et al.*, 2009; Ma and Berkowitz, 2011). The characterization of knockout mutants of CNGC-encoding genes provided the strongest genetic evidence for cAMP function in cellular Ca^{2+} increase, which was also demonstrated to be involved in plant defence responses (Clough *et al.*, 2000; Balagué *et al.*, 2003). In response to avirulent pathogens, cAMP elevation functioned upstream of reactive oxygen species (ROS) and nitric oxide (NO) production, through the direct modulation of CNGCs (Ma *et al.*, 2009, 2010).

Nevertheless, the pharmacological approach used so far to alter endogenous cAMP content does not taken into account the importance of the physiological concentrations of this secondary messenger and cannot rule out the existence of secondary effects related to the use of pharmacological compounds. This strategy cannot therefore fully reveal cAMP-dependent signalling mechanisms. Recently, a new genetic tool, namely the chimeric protein 'cAMP-sponge', has been successfully used in plants, specifically in tobacco Bright Yellow-2 cells, to study cAMP involvement in cell cycle progression and stress-related mechanisms (Sabetta *et al.*, 2016). The cAMP-sponge is constituted by the two-high affinity cAMP-binding domains of the human PKA Iβ regulatory subunit. The specific binding of cAMP to the sponge leads to cAMP sequestration, therefore reducing its intracellular levels (Lefkimmiatis *et al.*, 2009).

In this study, we generated *Arabidopsis thaliana* plants overexpressing the cAMP-sponge (cAS plants). The specificity towards cAMP of this genetic tool allowed the development of a more reliable and targeted approach than the pharmacological tool, to gain further insight into its role in plant defence response. The effect of *in vivo* cAMP dampening on defence responses and resistance was here evaluated following infection with the avirulent bacterial pathogen *Pseudomonas syringae* pv. *tomato* DC3000 carrying the avirulence gene *AvrB* (*PstAvrB*) that typically elicits an HR in *Arabidopsis thaliana* (Leister *et al.*, 1996). Bacterial growth, hypersensitive cell death and redox homeostasis were investigated in WT and cAS plants. Moreover, a large-scale comparative proteomic analysis was performed between the two genotypes and the

promoter regions of the genes encoding the differentially abundant proteins identified were further studied.

RESULTS

Arabidopsis thaliana Col-0 plants were transformed with the cAMP-sponge, by the floral dip method, and two stable independent transformed lines (cAS) was selected and characterized. Real-time polymerase chain reaction (PCR) analyses on the two homozygous lines revealed that the expression of the cAMP-sponge, was higher in the cAS3 line than in the cAS1 (Figure 1a). The expression of the cAMP-sponge protein in cAS plants was also confirmed *in vivo*, by means of confocal microscopy analyses, through the detection of the fluorescence of mCherry, which was fused to the sponge (see Experimental procedures). In accordance with the use of a constitutive promoter, the mCherry fluorescence was evenly distributed in cAS seedlings, i.e. cotyledon leaves, hypocotyl and roots (Figures 1b and S1). To check the efficiency of the cAMP-sponge in buffering cAMP, its content was measured in WT and transgenic cAS plants using the Alpha-Screen cAMP assay (see Experimental procedures). Both cAS lines showed the same total cAMP content than the WT plants (Figure 1c), likely to be because cAMP, bound to the cAMP-sponge, was released during the procedure of total cAMP extraction. By contrast, the measurement of free cAMP content showed significant differences, with transgenic cAS lines displaying around half of free cAMP compared with WT plants (Figure 1d). The specificity of the results obtained with Alpha-Screen method and the differences in free cAMP content among WT and cAS plants were confirmed with the widely used cAMP-Glo™ assay (Figure S2). The decrease in free cAMP was comparable in the two transgenic lines even though the expression level of the cAMP-sponge was different (Figure 1d). Despite the decrease in free cAMP, cAS plants did not show any observable gross phenotype in physiological conditions. Indeed, the same germination time, number, color and size of rosette leaves, as well as, time and height of inflorescence were observed between WT and transgenic lines (Figure S3).

In order to figure out whether a decreased amount of free cAMP could affect the ETI-mediated resistance, WT and cAS plants were infected with avirulent *PstAvrB*. Bacterial growth, 2 and 3 days post-infection (dpi), was slightly, but significantly, higher in the two cAS lines than in WT plants, as also evidenced by the increase in chlorotic areas, indicating a compromised resistance in cAS plants (Figure 2a,b). Moreover, the quantification of the hypersensitive cell death by ion leakage, in leaves infected with the avirulent *PstAvrB* showed that the reduction of cAMP content in cAMP-sponge-expressing lines led to a decrease in programmed cell death compared with WT plants (Figure 2c). To elucidate, at molecular level, if cAS plants were indeed affected in their ability to mount a full defence response, the expression of the well known defence marker gene *pathogenesis-related 1* (*PR-1*) was analysed after 24 h in leaves of WT and cAS plants infected with avirulent *PstAvrB*. Figure 2(d) shows that, according to the higher bacterial growth, the *PstAvrB*-induced upregulation of *PR-1* expression observed in WT plants was significantly reduced in cAS lines.

As both cAS lines showed the same phenotype in terms of resistance, partial impairment of HR cell death and lower *PR-1* induction, the cAS3 line (thereafter cAS) was selected for further molecular characterization of the responses of cAMP-sponge expressing plants to *PstAvrB* infection. Firstly, free cAMP content was measured in WT and cAS plants at 4 and 24 hpi with *PstAvrB* (Figure 3a). In WT plants, a progressive increase in free cAMP level occurred after infection, with a maximum observed at 24 hpi. By contrast, in the cAS line, an increase in free cAMP content was observed only at 24 hpi, although at lower levels with respect to WT plants (Figure 3a). As it has been previously reported that the cAMP produced in pathogen-inoculated Arabidopsis leaves could be responsible for cytosolic Ca^{2+} concentration elevation (Ma *et al.*, 2009), the cytosolic level of this secondary messenger was evaluated using the NES-YC3.6 Cameleon sensor (Krebs *et al.*, 2012). In WT plants, cytosolic Ca^{2+} increased at 4 hpi and returned to values comparable with mock-treated plants at 24 hpi. By contrast, the increase in cytosolic Ca^{2+} in cAS plants was evident only 24 h after infection with *PstAvrB*, suggesting a delay in cAS line response (Figure 3b). In the same manner, H_2O_2 rise, induced following plant infection with *PstAvrB*, was different in WT and cAS plants. At resting level (mock), H_2O_2 content was higher in cAS than in WT plants, suggesting that the low levels of cAMP could be sensed as a stress condition, as already reported by Sabetta *et al.* (2016). However, in WT plants, a significant increase in H_2O_2 content was observed at 4 hpi and this increased further at 24 hpi, whereas the H_2O_2 increase in cAS plants occurred only 24 h after infection with avirulent bacteria, and at higher level compared with WT plants. This finding further supports the hypothesis of a delayed defense response in plants displaying a lower cAMP content (Figure 3c). Such delay observed in the defence responses of cAS plants challenged with *PstAvrB* was supported by the analysis of total ascorbate (ASC) and glutathione (GSH) pools. Four hours after infection with *PstAvrB*, both antioxidants had already increased in WT plants, while their content did not change in cAS plants at the same time point. Conversely, an increase in both ASC and GSH occurred in infected cAS plants at 24 hpi (Figure 4a,b). However, ascorbate and glutathione redox state did not change in the two lines, neither under basal conditions, nor after infection (Figure S4). Consistently, the activities of dehydroascorbate reductase (DHAR)

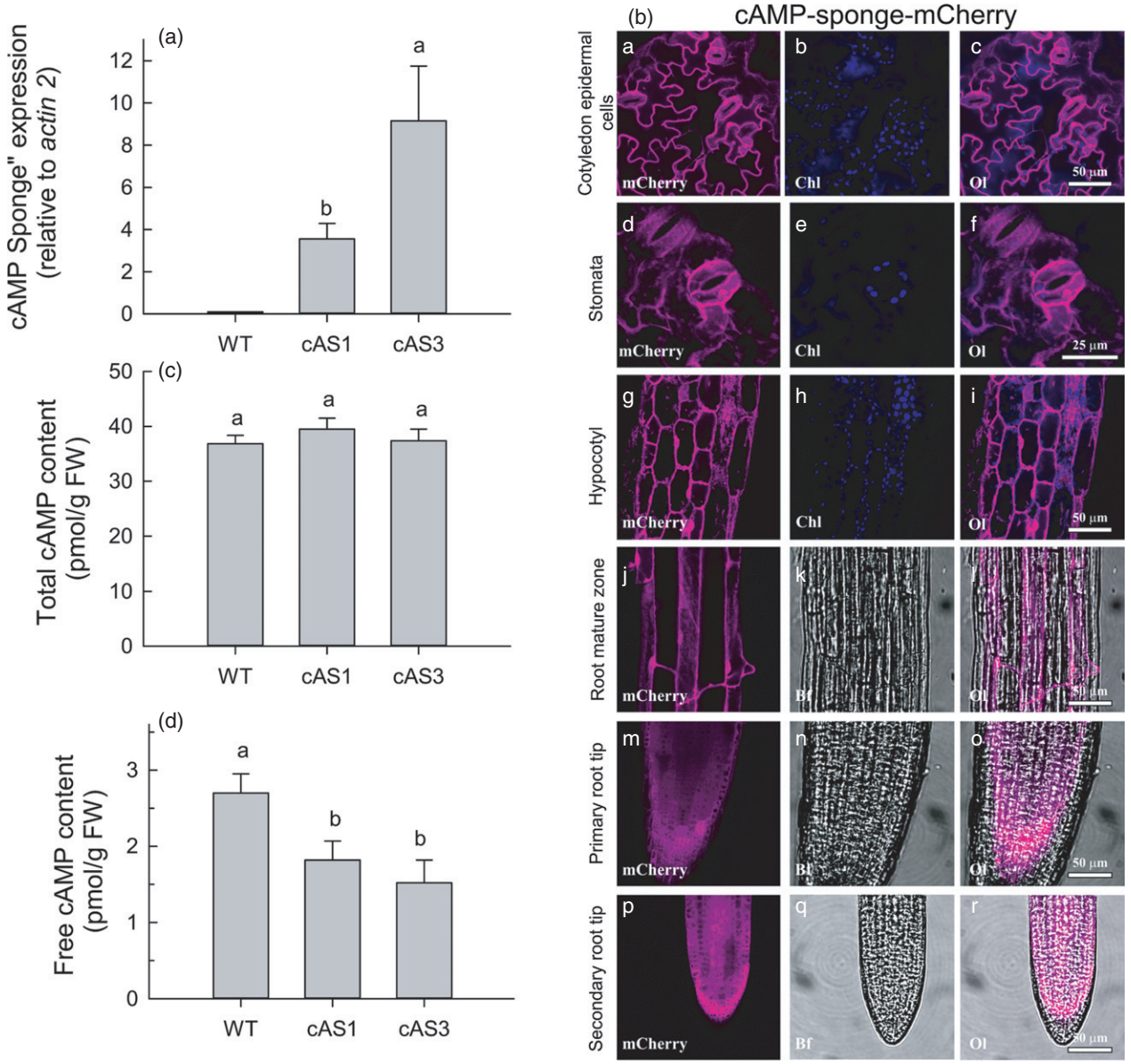

Figure 1. cAMP-sponge expression and cAMP content in WT and cAS lines.
(a) Transcript level of cAMP-sponge in WT and cAS lines. The expression level of cAMP-sponge was normalized to that of Actin2.
(b) Presence of cAMP-sponge protein visualized by mCherry fluorescence in a representative cAS3 10-day old seedling. (BA-BC) cotyledons; (BD-BF) stomata; (BG-BI) hypocotyl; (BJ-BL) root mature zone; (BM-BO) primary root tip; (BP-BR) secondary root tip. BA, BD, BG, BJ, BM, mCherry fluorescence in magenta; BB, BE, BH Chlorophyll (Chl) autofluorescence in blue; BK, BN, BQ Bright Field (Bf); BC, BF, BI, BL, BO, BR Overlay of the two channel shown for each tissue.
(c) Total and (d) free cAMP content in WT and cAS lines (see Experimental procedures). The values reported for cAMP-sponge expression and cAMP contents are the means ± standard errors from three biological replicates, each one with three technical replicates. Different letters indicate significant differences obtained by one-way ANOVA test ($P < 0.05$).

and glutathione reductase (GR), the enzymes involved in the reduction of the oxidized forms of ASC and GSH, respectively showed a similar behaviour in the two genotypes (Figure 4c,d). In particular, DHAR activity increased at 24 hpi in WT plants; at the same time point in cAS plants DHAR activity was already higher than that observed in WT plants under control conditions and did not change after inoculation (Figure 4c). Conversely, despite a rise in GR activity observed in both WT and cAS plants, such increase seems to occur earlier in cAS plants, in which it was observed at 4 hpi (Figure 4d). The total activity of ascorbate peroxidase (APX), the enzyme involved in H_2O_2 removal at the expense of ASC, significantly increased in WT plants 4 and 24 h after inoculation with *PstAvrB*. By contrast, in cAS plants, total APX activity rose only at 24 hpi, reaching a higher level compared with

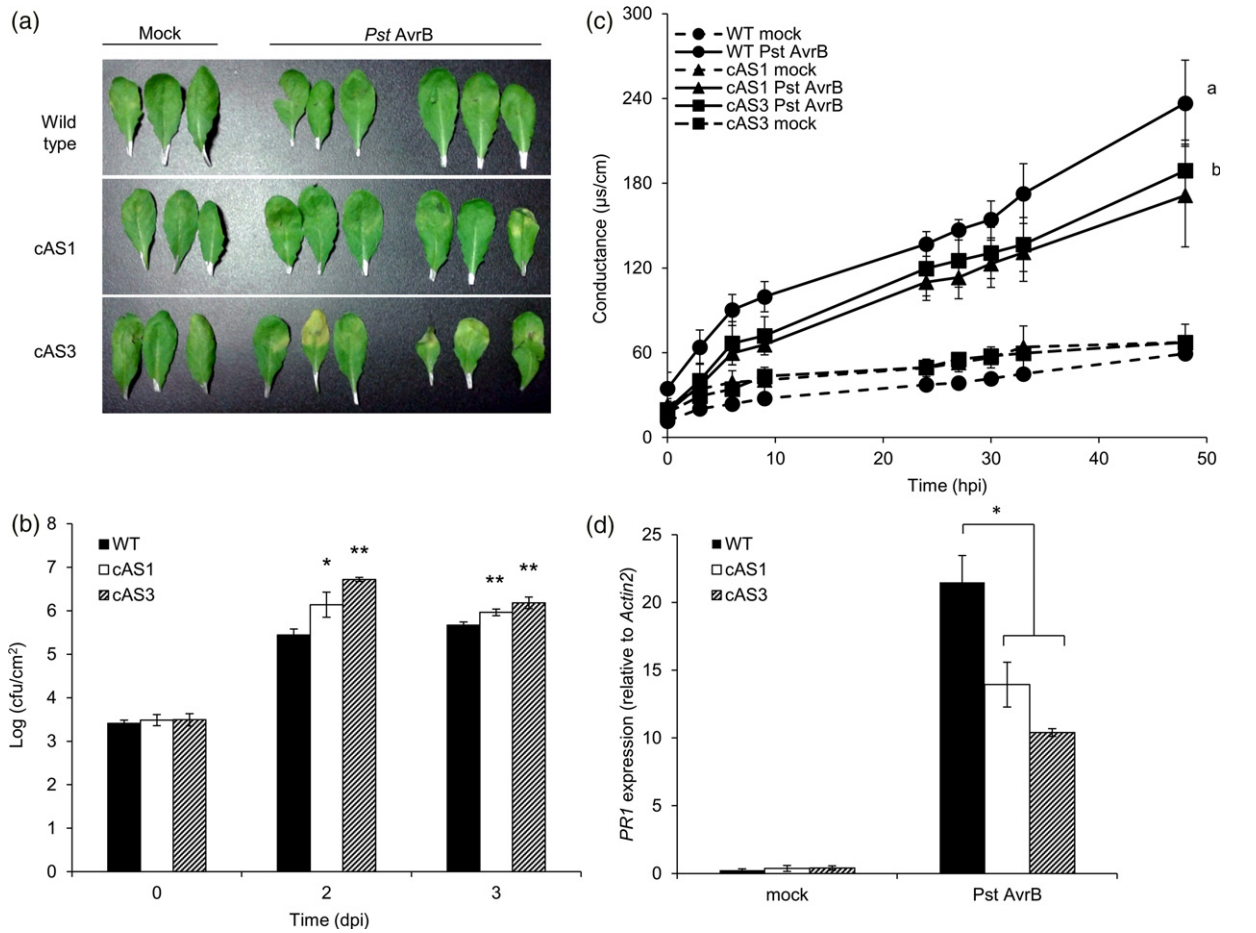

Figure 2. The genetically lowering of cAMP affects local resistance and hypersensitive cell death.
(a) Representative images of leaves from WT, cAS1 or cAS3 plants at 3 days post-infection (dpi) with avirulent *PstAvrB* (5×10^5 cfu mL^{-1}).
(b) Plant resistance assessed by analysis of bacterial growth kinetics in plants following the infection of *A. thaliana* WT, cAS1 or cAS3 plants with avirulent *PstAvrB* (5×10^5 cfu mL^{-1}) at 2 and 3 dpi.
(c) Hypersensitive cell death quantified by ion leakage on leaf disks derived from WT, cAS1 or cAS3 plants and infiltrated with *PstAvrB* (10^7 cfu mL^{-1}). Conductance was recorded up to 48 h.
(d) Expression level of *PR-1* in leaves from WT, cAS1 and cAS3 plants, collected at 24 hpi with *PstAvrB* (10^7 cfu mL^{-1}). The expression level of *PR1* gene was normalized to that of *Actin2*. In each experiment, mock-infiltrated plants were used as controls. Values are means ± SE of three biological replicates and experiments were repeated at least twice with similar results. For expression analysis three technical replicates were included for each biological replicate. Asterisks indicate a statistical difference ($P < 0.05$) according to Student's *T* test.

WT plants at the same time point (Figure 5a). The expression of different APX isoenzymes at 24 hpi showed that the transcript level of cytosolic *APX1* and *APX2* increased after infection with *PstAvrB* in both WT and cAS plants. However, inducible *APX2* upregulation was higher in WT than in cAS plants (Figure 5b). Conversely, the chloroplastic isoenzymes showed a different behaviour following *PstAvrB* infection, with the expression of *sAPX* and *tAPX* increasing and decreasing, respectively, in both WT and cAS lines following challenge with avirulent bacteria (Figure 5b).

To get deeper insights into molecular changes related to the lower content of free cAMP in cAS plants, a large-scale proteomic analysis was performed 24 h following plant infection with *PstAvrB*. Figure 6 shows the main features of the proteome in cAS line compared with WT plants, both at resting level and after infection. The lower free cAMP content in cAS plants only slightly affected the proteomic profile at resting level. Indeed, only four differentially accumulated proteins (DAPs) were found in cAS plants compared with WT plants. In particular, the phosphoglycerate dehydrogenase 1 (AT4G34200) and the chlorophyllase 1 (AT1G19670) were upregulated in cAS plants, with a $\log_2$ fold change ($\log_2$FC) of 1.18 and 1.1, respectively, whereas Spiral1 (AT2G03680) and phospholipase C2 (AT3G08510) were downregulated in transgenic plants, with a $\log_2$FC of −3.2 and −13.06, respectively. After infection with *PstAvrB*, 65 and 91 DAPs were found in WT and cAS plants, respectively. A core of 49 proteins, mainly related to defence responses, was modulated in

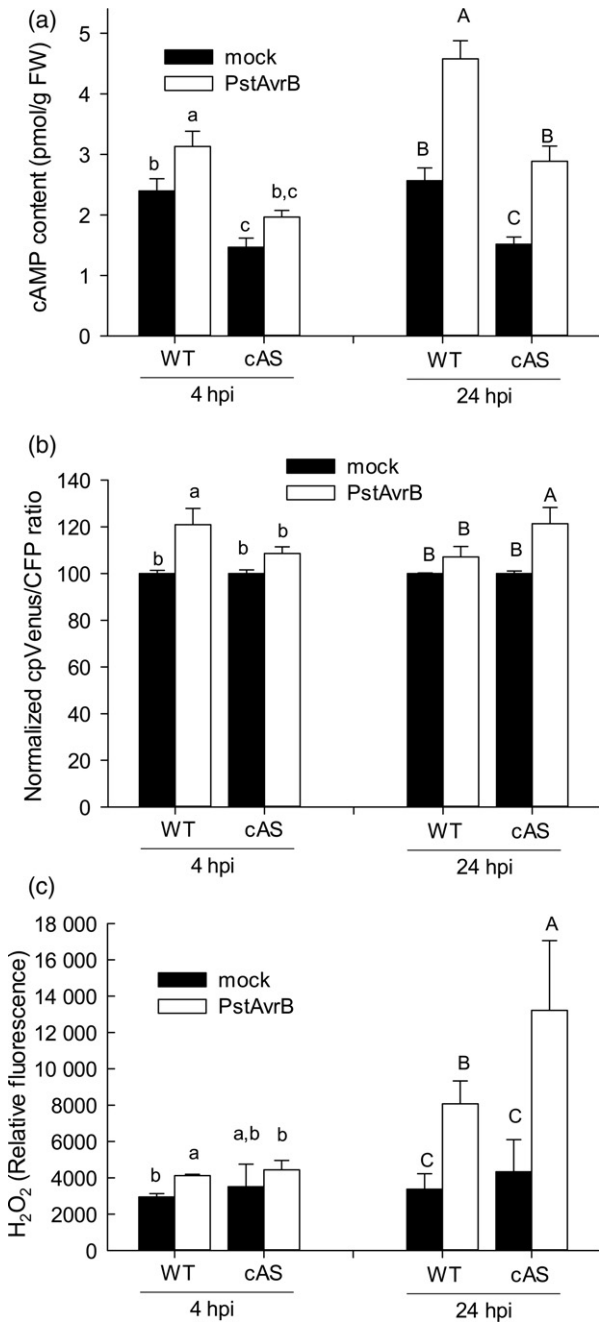

Figure 3. The failure in cAMP elevation after infection with *PstAvrB* in Arabidopsis cAS plants altered Ca^{2+} and H_2O_2 homeostasis.
(a) cAMP, (b) Ca^{2+} and (c) H_2O_2 levels in leaves of WT, cAS plants infected with *PstAvrB* (10^7 cfu mL^{-1}) at 4 and 24 hpi. In each experiment, mock-infiltrated plants was used as controls. WT and cAS plants expressing the NES-YC3.6 Ca^{2+} sensor were used to determine Ca^{2+} levels by imaging as described in Experimental procedures. Values are means ± SE of at least three biological replicates, each one with three technical replicates. Different letters indicate a statistical difference ($P < 0.05$) according to ANOVA test.

both genotypes (Figure 6, Table S1), while 16 and 42 unique DAPs were unique to WT and cAS lines, respectively (Figure 6, Tables S2 and S3).

The comparison of infected cAS and WT plants revealed 18 DAPs, of which 10 were upregulated and eight were downregulated in the cAS line (Table S4). In particular, seven of the 10 upregulated proteins belonged to functional categories related to transport and photosynthesis and three of these have an unknown function. Conversely, the downregulated proteins are involved in redox control, translation and metabolism.

To verify whether the proteins uniquely accumulated in WT plants after infection were enriched for specific consensus sequences in their promoter regions putatively dependent on cAMP, several *de novo* motif analysis tools were used (Bailey *et al.*, 2009; Nguyen *et al.*, 2018). Comparing the results of different algorithms, 10 of the 12 genes coding for the proteins uniquely upregulated in WT plants, showed the CGCG motif (found by MEME with E-value 4.0e+002, RSAT Plants Oligo analysis with E-value of 6.8e-01) as recurring (Figure 7a,b). Compared with random intergenic sequences, CGCG motif showed approximately two-fold enrichment ($P < 0.001$; using RSAT Plants matrix scan). The intergene regions of all the genes of this group showed the presence of at least one copy of the CGCG pattern (Figure 7c). A further analysis of such motif figured out that the CGCG pattern is similar to the pattern known as AtSR1 target (E-value 8.4374e-05) (Mahony and Benos, 2007). Interestingly, and in line with our results, the interrogation of transcription databases revealed that the genes coding for the proteins uniquely accumulated in WT plants after infection, and containing the CGCG motif, were downregulated with respect to the WT in the negative dominant *sr1-4D* mutant (also known as *camta3D*) after the treatment for 1 h with flg22 or 4 h after infection with avirulent *Pst AvrRpm1* or *Pst AvrRps4* (Table S5; Maekawa *et al.*, 2017; Jacob *et al.*, 2018). The expression of five of these genes (*PUB13*, *PDI10*, *DJ1E*, *CRK14* and *HSP90*) was therefore analysed in WT and cAS plants at 4 and 24 h after *PstAvrB* infection, by real-time qPCR. The expression of HSP90 did not differ significantly between WT and cAS plants both at 4 and 24 hpi. Conversely, the fold changes in the transcript levels of *PUB13*, *PDI10*, *DJ1E* and *CRK14* were significantly lower in cAS than in WT plants at 4 hpi (Figure 7d), therefore strongly supporting an alteration of protein accumulation in cAS plants through AtSR1 mis-regulation.

DISCUSSION

Numerous indications suggest the involvement of cAMP in plant defence mechanisms against pathogens. An increase in intracellular cAMP content has been reported in different plants treated with elicitors of defence responses (Bolwell, 1992; Kurosaki and Nishi, 1993; Cooke *et al.*, 1994; Zhao *et al.*, 2004; Jiang *et al.*, 2005; Ma *et al.*, 2009; Lu *et al.*, 2016). However, as little information is known on enzymes responsible for cAMP synthesis and degradation in plants,

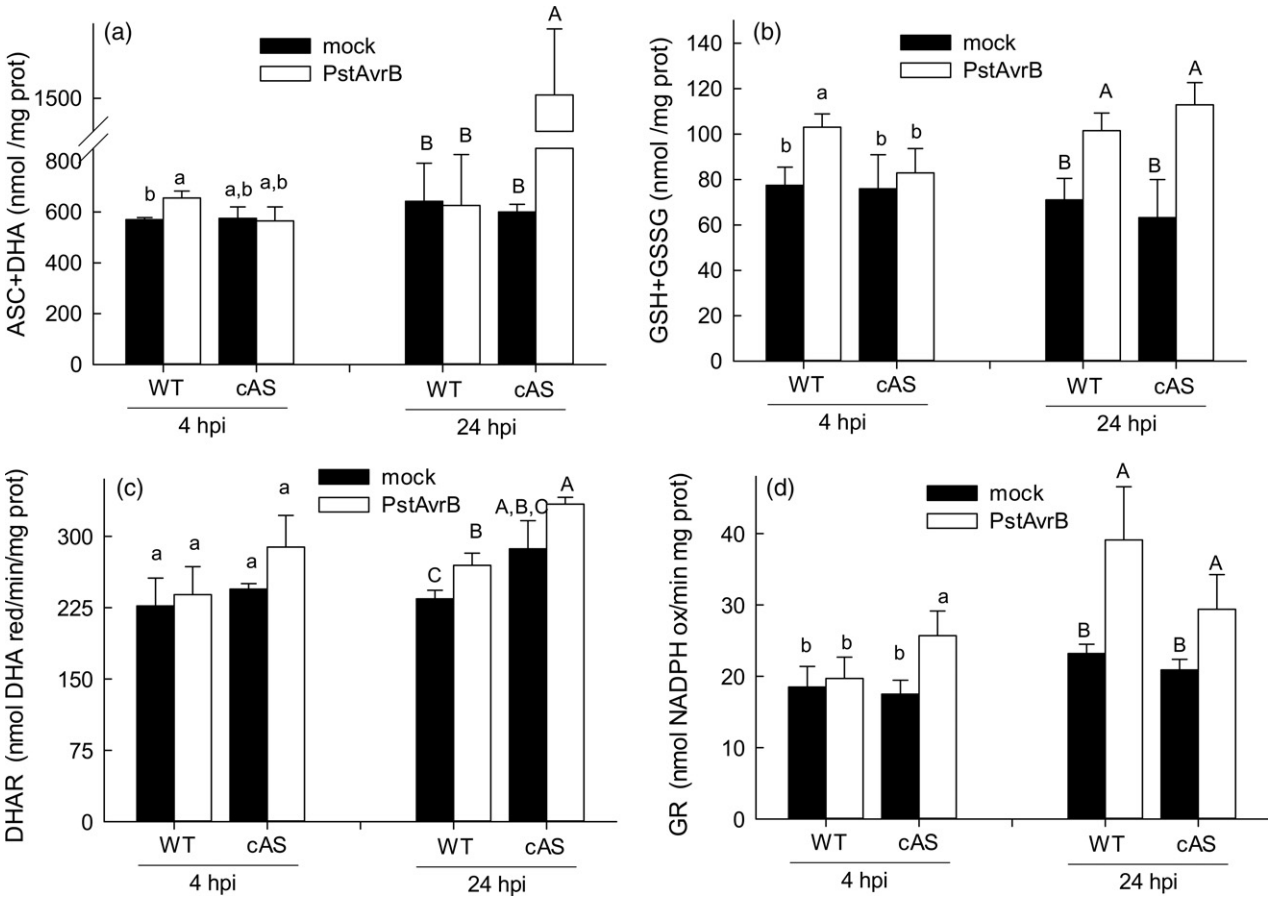

Figure 4. Ascorbate and glutathione metabolism in Arabidopsis WT and cAS plants in control conditions (mock) and after infection with *PstAvrB*. Arabidopsis WT and cAS plants were infected with *PstAvrB* (10^7 cfu mL^{-1}) and leaf samples were collected for analysis. The total ascorbate pool (a; ASC + DHA) and glutathione pool (b; GSH + GSSG) were measured at 4 and 24 hpi. The activity of the dehydroascorbate reductase (c) and glutathione reductase (d) were measured in total protein extracts. In each experiment, mock-infiltrated plants were used as controls. Values are means ± SE of at least three biological replicates, each one with three technical replicates. Different letters indicate a statistical difference ($P < 0.05$) according to ANOVA. GSH, reduced glutathione; GSSG, oxidized glutathione; ASC, ascorbate; DHA, dehydroascorbate; DHAR, dehydroascorbate reductase; GR, glutathione reductase.

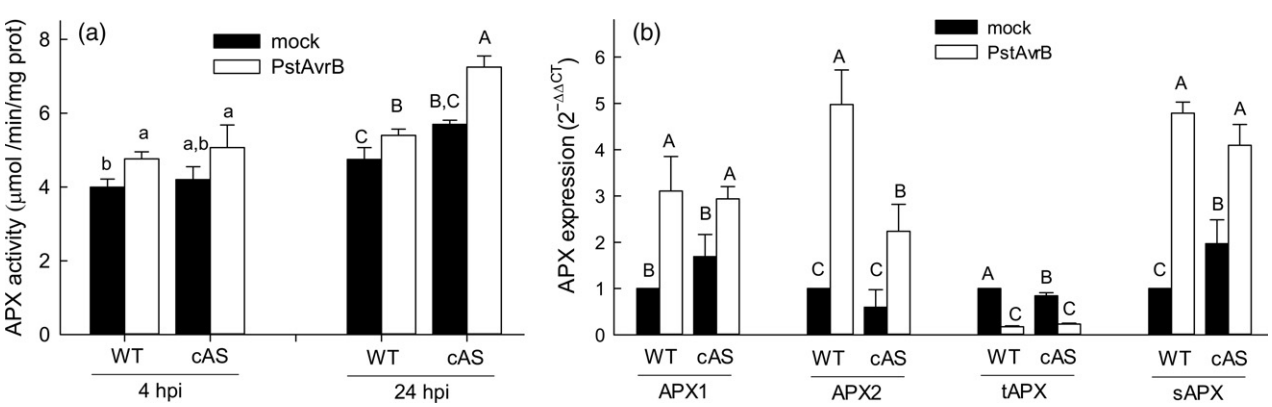

Figure 5. Ascorbate peroxidase is differently affected in Arabidopsis WT and cAS plants after infection with *PstAvrB*. WT and cAS plants were infiltrated with *PstAvrB* (10^7 cfu mL^{-1}) and leaf samples was collected 4 and 24 hpi for the analysis of the APX enzymatic activity (a) in total protein extracts. In each experiment, mock-infiltrated plants were used as controls. Leaf samples were collected 24 hpi for analysis of the expression of different APX isoenzymes by real-time RT-PCR using gene-specific primers (b). The expression level of *APX1*, *APX2*, *sAPX* and *tAPX* was normalized to that of *GAPC2*; the values obtained for infected WT and cAS plants (mock and *PstAvrB*-treated) were normalized with values of WT mock samples, which were fixed to one in each biological replicate. Values are means ± SE of at least three biological replicates, each one with three technical replicates. Different letters indicate a statistical difference ($P < 0.05$) based on ANOVA. *APX1*, cytosolic ascorbate peroxidase; *APX2* inducible cytosolic ascorbate peroxidase; *sAPX*, stromal ascorbate peroxidase; *tAPX*, thylakoidal ascorbate peroxidase.

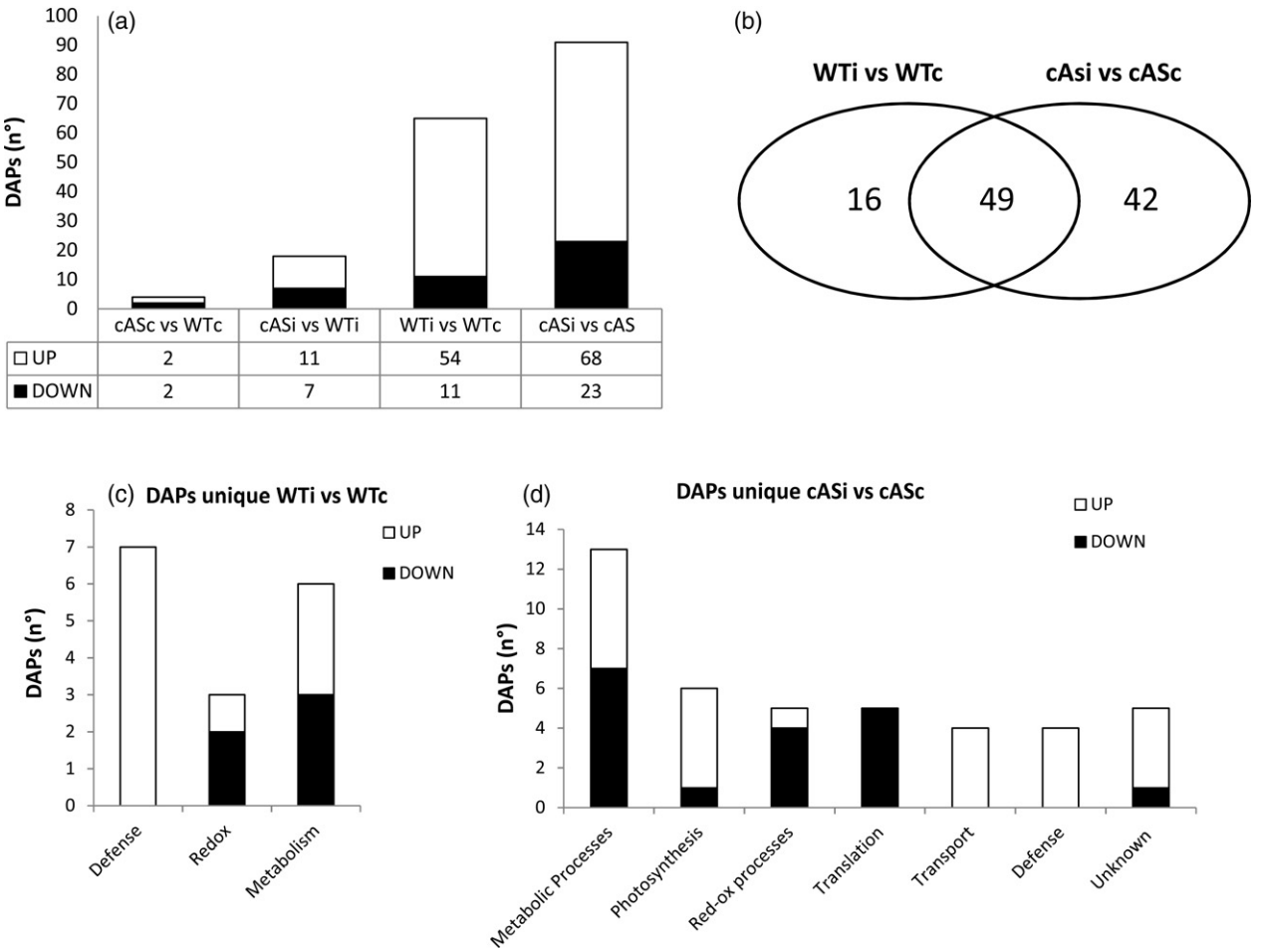

Figure 6. Low level of cAMP in cAMP-sponge expressing plants affects the proteomic pattern of Arabidopsis plants in response to *PstAvrB*.
(a) The number of differentially accumulated proteins (DAPs) in cAS plants compared with WT plants under basal conditions and following infection with *PstAvrB* (10^7 cfu mL^{-1}). White bars represent upregulation and black bars downregulation.
(b) Venn diagram showing the number of unique and common DAPs in cAS and WT plants following infection at 24 hpi with *PstAvrB* (10^7 cfu mL^{-1}).
(c) Functional category distribution of unique differentially accumulated proteins following the infection of WT plants with *PstAvrB* (10^7 cfu mL^{-1}) compared with mock-infiltrated plants.
(d) Functional category distribution of differentially abundant proteins in infected cAS plants compared with mock-infiltrated plants.

the study of cAMP-mediated signalling pathways in plant defence has always relied on the use of cell-permeable cAMP analogues and stimulators or inhibitors of mammalian ACs and PDEs (Gehring and Turek, 2017). In order to study the specific cAMP-dependent pathways in plant immune response, we used here a genetic approach by overexpressing the cAMP-sponge, which specifically binds cAMP (Lefkimmiatis *et al.*, 2009). Transgenic cAS plants accumulate lower levels of free cAMP compared with WT, confirming the efficiency of the sponge to buffer cAMP in plants, as previously demonstrated in tobacco BY-2 cells (Sabetta *et al.*, 2016). At resting level, cAS plants are not phenotypically altered in comparison with WT plants and their proteome profiles differ only by four DAPs, among which the phospholipase C2 (PLC2), which is almost undetectable in cAS line. These observations support a non-pleiotropic effect of cAMP-sponge and the specificity of our approach. By contrast, the decrease in cAMP content in cAS plants led to a reduced resistance of the transgenic lines to the avirulent pathogen *PstAvrB*, associated with an impairment in hypersensitive cell death. More recently, a leucine-rich repeat protein with adenylyl cyclase activity (AtLRRAC1) has been identified in *Arabidopsis thaliana* (Bianchet *et al.*, 2019). Interestingly, and in line with our results, knockout mutants of AtLRRAC1 showed compromised immune responses to *Pseudomonas syringae* (Bianchet *et al.*, 2019). The inoculation of Arabidopsis plants with avirulent strains of *Pseudomonas syringae* pv. *tomato* DC3000 carrying avirulence genes was previously reported to trigger cAMP concentration elevation, further reduced in the presence of mammalian AC inhibitors (Ma *et al.*, 2009). In this study, we confirmed that, in WT plants, an increase

(a)

Gene ID	TAIR Functional description	Log_2FC
AT4G08850	Leucine-rich repeat receptor- like protein kinase	3,71
AT1G04980	**Protein disulfide-isomerase 10 (PDI10)**	3,03
AT5G52640	**Heat shock protein 90-1 (HSP90)**	2,24
AT2G38860	**DJ-1 protein homolog E (DJ1E)**	2,03
AT3G46510	**Plant U-BOX 13 (PUB13)**	1,61
AT3G60130	Beta-glucosidase 16	1,52
AT4G23220	**Cysteine-rich receptor-like protein kinase 14 (CRK14)**	1,44
AT3G19010	2-Oxoglutarate and Fe(II)-dependent oxygenase	1,33
AT2G01490	Phytanoyl-CoA 2-hydroxylase	1,19
AT1G77510	Protein disulfide isomerase 6	1,04

(b)

A	0	0	11	0	0	0	0	0	8	2
C	9	5	0	10	3	9	4	3	0	6
G	2	4	0	0	8	0	7	6	0	0
T	0	2	0	1	0	2	0	2	3	3

(c)

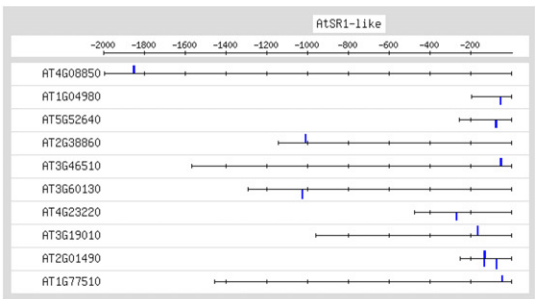

(d)

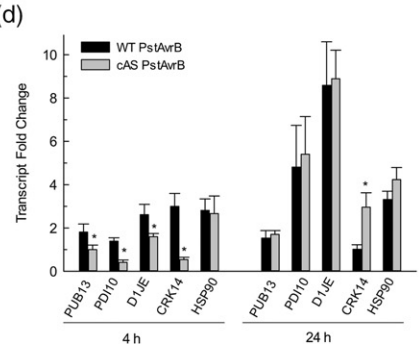

Figure 7. *In-silico* analysis of the promoters and expression level of the genes coding for proteins uniquely accumulating in WT plants in response to *PstAvrB*. The CGCG BOX-like DNA motif was found using MEME (E-value 4.0e+002) and RSAT Plants Oligo analysis (E-value of 6.8e-01) to be the recurring consensus sequence.

(a) List of proteins with CGCG BOX-like motif.

(b) Position weight matrix (PWM) and its WEB Logo graphic representation. The overall height of each stack indicates the conservation of the sequence at that position and the bit score indicates the relative frequency of the corresponding nucleotide.

(c) Scanning of the intergenic regions of the same group of genes using RSAT Plants matrix scan. All the genes show the presence of at least one copy of the CGCG BOX-like.

(d) Fold change in the transcripts level of *PUB13*, *PDI10*, *DJ1E*, *CRK14* and *HSP90* after 4 and 24 h of infection with *PstAvrB* in WT and cAS plants. The expression level of the selected genes was normalized to that of *Actin2*. The values obtained for infected WT and cAS plants were normalized with the values of their respective controls (mock-treated), which were fixed to 1 in each biological replicate. Values are means ± SE of three biological replicates, each one with two technical replicates. Asterisks indicate a statistical difference ($P < 0.05$) according to Student's *T* test.

in cAMP production occurred at 4 hpi and this elevation increased further at 24 hpi. The genetically controlled lowering of free cAMP in cAS plants significantly delayed the HR induced by *PstAvrB*, confirming that this secondary messenger is needed for the correct immune response activation. Cytosolic Ca^{2+} increase, which represents a crucial event during the signalling related to plant–pathogen interaction (Dangl *et al.*, 1996; Grant *et al.*, 2000), is severely impaired in cAS plants. In particular, these plants, displaying lower free cAMP levels after pathogen infection, showed a significant delay of the sustained cytosolic Ca^{2+} increase that was not observable at 4 hpi and appeared only at 24 hpi, when in WT plants the Ca^{2+} content had already returned to values comparable with mock-treated plants. Several defence mechanisms are dependent on Ca^{2+} signalling, among which is salicylic acid (SA) biosynthesis in plant immunity (Zhang *et al.*, 2010, 2014; Nomura *et al.*, 2012). In line with a possible role for cAMP in SA-dependent plant defence responses (Jiang *et al.*, 2005), the upregulation of SA-dependent *PR-1* gene expression was lower in cAS than in WT plants. It is therefore tempting to assume a possible regulation of the SA-dependent pathway by cAMP through cytosolic Ca^{2+} homeostasis modulation. Much evidence indicates that cAMP permits Ca^{2+} entrance into plant cells through CNGCs, initiating that the signalling event cascades occurred in response to biotic stress (Clough *et al.*, 2000; Balagué *et al.*, 2003; Jurkowski *et al.*, 2004; Yoshioka *et al.*, 2006; Ali *et al.*, 2007; Chin *et al.*, 2013; Lu *et al.*, 2016). Our data suggested that the delay in HR activation could be in part due to a failure in the activation of CNGCs in cAS plants, although we cannot exclude a possible downregulation of Ca^{2+} efflux transporters in our system (Bose *et al.*, 2011). It must also be considered that a recent paper indicates that AtCNGC2, which was predicted to mediate Ca^{2+} influx into the cytosol in response to pathogen infection (Ali *et al.*, 2007), plays a role in the transport of Ca^{2+} from veins to leaf cells but it is not directly involved in HR establishment (Wang *et al.*, 2017). Conversely, it is known that cytosolic Ca^{2+} elevation in response to several elicitors of plant defence involves, in

part, phosphatidylinositol-specific PLCs (Lecourieux *et al.*, 2006). Interestingly, PLC2, the most abundant plasma membrane PLC isoform, in common, strongly and constitutively expressed (Pokotylo *et al.*, 2014), is heavily downaccumulated in cAS plants. In this context, the absence of PLC2 in cAMP-sponge expressing lines could be involved in the failure of Ca^{2+} entrance into cells. Lacking the correct Ca^{2+} modulation, plants could not be able to activate the suitable response to a given stress, and consequently do not acclimate to the new conditions, compromising their survival (Lenzoni *et al.*, 2018). Accordingly, the delayed raise in cytosolic Ca^{2+} would not allow cAS plants to initiate the suitable defence response, consequently affecting resistance.

During the infection with avirulent pathogens, plants induce a biphasic ROS accumulation characterized by a low-amplitude transient first phase and followed by a second phase, with a higher and continued increase in ROS, which precedes HR (Levine *et al.*, 1996; Bolwell *et al.*, 2002; Torres *et al.*, 2006). While WT Arabidopsis plants show a clear increase in H_2O_2 at 4 hpi, followed by a sustained accumulation at 24 hpi, the cAMP impairment in cAS plants caused an altered ROS production with a delay in H_2O_2 increase especially at the early stage. It has been reported that the increase in cytosolic Ca^{2+}, due to the increased level of cAMP, is needed for ROS production in both bean and *Arabidopsis* cell cultures (Bindschedler *et al.*, 2001; Davies *et al.*, 2006). Ca^{2+} raise upon pathogen recognition could directly activate ROS production by increasing NADPH oxidase activity or extracellular peroxidases, required for the appropriate apoplastic oxidative burst (Bindschedler *et al.*, 2001; Sagi and Fluhr, 2006; Camejo *et al.*, 2016). Moreover, the low level of PLC2 in cAS plants could also contribute to the compromised H_2O_2 increase in the first phase of pathogen infection. Indeed, PLC2-silenced Arabidopsis plants show compromised ROS production and ROS-dependent responses upon flg22 treatment (D'Ambrosio *et al.*, 2017). The recognition of the fungal protein Avr4 by the resistance protein Cf-4 in tomato cells induces a rapid activation of PLC leading to the production of phosphatidic acid (PA) that, in turn, is responsible for the oxidative burst (de Jong *et al.*, 2004). In the same way, in Arabidopsis, the perception of two *Pseudomonas syringae* Avr proteins, namely AvrRpm1 and AvrRpt2 by their cognate resistance proteins RPM1 and RPS2, respectively, cause a biphasic accumulation of PA, the first of which is due to PLC activity (Andersson *et al.*, 2006). PA can further interact directly with the NADPH oxidase RBOHD (Respiratory Burst Oxidase Homolog D), therefore enhancing ROS production (Zhang *et al.*, 2009). Finally, PLC2 was reported to be associated with RBOHD, and it was proposed that the secondary messengers derived from PLC2 activation, i.e. PA and/or the indirect increase in cytosolic Ca^{2+}, could positively stimulate NADPH oxidase activity (D'Ambrosio *et al.*, 2017). A similar scenario could also occurs in cAS plants, in which the lack of PLC2 could be linked with impaired Ca^{2+} variations and H_2O_2 production.

ROS accumulation into plant cells depends on the delicate equilibrium between ROS production and scavenging at the correct time (Paciolla *et al.*, 2016) and the redox impairment observed in cAS plants seems to be also due to the alteration in the scavenging pathways. Increase in antioxidant defences has been reported as a general mark correlated with pathogen resistance (De Gara *et al.*, 2003; Kuzniak and Sklodowska, 2004; Faize *et al.*, 2012; Lanubile *et al.*, 2012). Consistently, in Arabidopsis WT plants, ASC, GSH and total APX activities increased already at 4 hpi together with the increase in H_2O_2, while in cAS plants the increase in these ROS scavengers is evident only at 24 hpi. Few evident changes between WT and cAS plants have been observed at 24 hpi in the expression of genes encoding the different *APX* isoenzymes. The most important difference concerns *APX2*, whose expression in response to bacterial infection was higher in WT than in cAS plants. This is not surprising as *APX2* has been reported to be induced by several kinds of stress (Karpinski *et al.*, 1999; Gorecka *et al.*, 2014; Locato *et al.*, 2018). The increase in APX activity, which is more evident, even if delayed, in cAS plants, could be due to post-transcriptional modifications that affect this enzyme under oxidative conditions (de Pinto *et al.*, 2013, 2015).

The failure in GSH increase at the early stage of infection could also contribute to the altered signalling in infected cAS plants leading to compromised *PR-1* expression and resistance. Indeed, Arabidopsis mutants displaying altered levels of GSH demonstrated an inverse correlation between GSH content and resistance to pathogens (Parisy *et al.*, 2007). Moreover, an increased GSH content, due to the exogenous application of GSH or to the overexpression of the γ-glutamylcysteine synthetase, activates defence-related genes, including *PR-1* (Wingate *et al.*, 1988; Senda and Ogawa, 2004). Accordingly, GSH plays a key role in the redox regulation and nuclear accumulation of NONEXPRESSOR OF PATHOGENESIS-RELATED GENES 1 (NPR1), the SA-responsive transcriptional co-activator of defence genes (Mou *et al.*, 2003; Dong, 2004; Tada *et al.*, 2008; Kovacs *et al.*, 2015). Interestingly, cAS plants compared with WT plants also showed a lower accumulation of nitrosoglutathione reductase (GSNOR) at 24 hpi. This could further compromise cAS resistance against *PstAvrB* through SA synthesis and/or signalling impairment or by promoting NPR1 oligomer formation due to its excessive *S*-nitrosylation (Dong, 2004; Feechan *et al.*, 2005; Malik *et al.*, 2011).

The infection of cAS plants leads to an accumulation of different light harvesting proteins, principally the ones of photosystem II. Interestingly, a similar behaviour has been

observed in *atgsnor* knockout plants, which also showed an altered response to the avirulent pathogen (Holzmeister *et al.*, 2011). Such enrichment in proteins of the photosynthetic process in cAS plants, could favour the maintenance of photosynthesis and consequently the bacterial growth. Indeed, genes involved in photosynthesis are usually downregulated during plant–pathogen interaction and this decrease is more marked with avirulent pathogens, probably because the impairment in photosynthesis reduces sugar production to limit the energy necessary for rapid pathogen growth (Zou *et al.*, 2005; Bolton, 2009; Rojas *et al.*, 2014). It has also been shown that PsbS deficiency leads to a high PSII-driven superoxide production to counteract the lack of qE (Zulfugarov *et al.*, 2014). Therefore, alternatively, increase in PSII-related proteins could allow cAS plants to compensate the compromised redox state, in particular H_2O_2 production, which is absent in the early phase of the infection and rises at 24 hpi.

The proteomic study showed that many of the defence proteins accumulate in both WT and cAS plants at 24 hpi with *PstAvrB*, underlining the idea that the alteration of the response observed in cAS plants could be due to a delay in the timing of the response rather than to a failure in its activation. However, seven defence proteins uniquely accumulated in WT plants after infection. Among these proteins we found HSP90, which is strongly involved in the stabilization of resistance proteins and required for correct defence signal transduction (Shirasu, 2009). Another protein that uniquely accumulated in WT plants was cysteine-rich receptor-like kinases 14 (CRK14), whose expression is induced by flg22 treatment; in accordance with impairment of immune response in cAS plants, where CRK14 does not accumulate, silencing of CRKs caused enhanced susceptibility to *Pseudomonas syringae*. Moreover, a possible involvement of CRKs in cell death was also suggested (Yadeta *et al.*, 2017). The failed accumulation of DJ1E, which is involved in glutathione metabolism and in the synthesis of phytoalexins (Zhou and Freed, 2005; Wei *et al.*, 2006), may also account for the higher susceptibility of cAMP-sponge expressing plants. Interestingly, the DJ1E promoter is strongly responsive to both necrotizing and non-necrotizing elicitors and a mechanism has been proposed for its regulation involving two AP2/ERF transcription factors acting antagonistically, namely ORA59 (induction) and ERF10 (repression) (Lehmeyer *et al.*, 2016). Given the regulation of ORA59 and ERF10 by jasmonate and SA/ethylene, respectively (Pré *et al.*, 2008; Caarls *et al.*, 2017), and in line with a lower induction of *PR-1*, this finding may suggest an impairment in hormone-related pathways in cAS plants, therefore providing a link between cAMP and hormones in plant defense responses.

In addition to *cis*-regulatory elements modulated by hormones like in *DJ1E* promoter, the regulatory regions upstream of the genes coding for proteins uniquely accumulating in infected WT plants at 24 hpi share a CGCG motif, bound by AtSR1, a calcium-dependent calmodulin-binding transcription factor, for repressing target gene expression (Yang and Poovaiah, 2002; Du *et al.*, 2009). Interestingly, these genes are less expressed with respect to the WT in the negative dominant *sr1-4D* mutant in the first phases of treatment with flg22 and infection with the avirulent *Pst AvrRpm1* or *Pst AvrRps4* bacteria (Table S5; Maekawa *et al.*, 2017; Jacob *et al.*, 2018), as well as in cAS plants at 4 hpi with *Pst AvrB*. These data support a link between cAMP and AtSR1 function and indicate that, in cAS plants, the low availability of cAMP could be responsible for an incorrect temporal modulation of the AtSR1 function, blocking in an inopportune moment the transcription of the genes controlled by this TF.

Our data confirmed that changes in the timing and levels of defence signals involved in PTI and ETI affected the speed and strength of these immune responses and the proper regulation of defence genes (Tsuda *et al.*, 2008; Katagiri and Tsuda, 2010; Birkenbihl *et al.*, 2017). The variations in free cAMP content and in the timing and levels of signals upon pathogen perception, likely also to be through the mis-regulation of the AtSR1 activity, affected the right activation of an efficient immune response.

In addition to change in gene expression and protein abundance, we cannot rule out the role of phosphorylation or other post-translational modifications in cAMP-mediated signalling. This issue, as well as the relationship between cAMP, ROS and Ca^{2+}-dependent signalling pathways will be studied more in depth based on the results reported in this work.

EXPERIMENTAL PROCEDURES

Plant material and growth conditions

Arabidopsis thaliana ecotype Columbia [Col-0] seeds was surface sterilized and germinated on Murashige and Skoog (MS) plates (Murashige and Skoog, 1962) containing 1% sucrose and 0.8% agar in a growth chamber (250 μmol photons m^{-2} sec^{-1}; 22°C) under a long-day regime (16 h of light/8 h of dark) and 70% relative humidity. After cold treatment for 2–3 days, plates were transferred to a growth chamber, and seedlings were transferred when they were 10–12 days old to soil in a climate-controlled chamber under the same photoperiod. For the selection of transgenic plants, seeds were germinated as for WT plants in Petri dishes supplemented with 50 mg L^{-1} kanamycin. To analyse the accumulation of cAS mRNAs, leaves were collected 2–4 weeks after germination and immediately frozen in liquid nitrogen until use.

Generation of *Arabidopsis thaliana* plants expressing the cAMP-sponge construct

The construct containing the C-terminus of the regulatory subunit RIβ of the human protein kinase A (PKA) tagged with the mCherry reporter gene, named cAMP-sponge (ΔNH_2PKARIβ-mCherry, Lefkimmiatis *et al.*, 2009), was kindly provided by Prof. M. Hofer from the Boston Healthcare System and the Department of Surgery, Brigham and Women's Hospital and Harvard Medical School

of Massachusetts, MA, USA. It was initially transferred to the pENTR™/D/TOPO^R Vector (Invitrogen, USA), between the cauliflower mosaic virus (CaMV) 35S promoter and the NOS terminator sequences using the primers indicated in Table S5). The pENTR™/D/TOPO^R Vector carrying the cAMP-sponge was then recombined with the pK2GW7Gateway™ destination vector (Karimi *et al.*, 2002), conferring plant kanamycin resistance. The pK2GW7::cAMP-sponge construct was sequenced in order to confirm the absence of PCR-induced nucleotide changes and the correct orientation. Plasmid DNA (10 ng) was introduced into *Agrobacterium tumefaciens* GV3101 (pMP90) competent cells by electroporation. Spectinomycin, rifampicin, tetracycline and gentamycin at final concentrations of 100, 50, 5 and 25 μg mL^{-1}, respectively, were used to select transformed colonies. The recombinant *A. tumefaciens* GV3101 strain harbouring the pK2GW7::cAMP-sponge plasmid or the empty vector was used to stably transform Arabidopsis plants according to the floral dip method (Clough and Bent, 1998). Stable insertion of the exogenous expression cassette was checked in kanamycin-resistant Arabidopsis plants by genomic DNA PCR amplification with primers for the neomycin phosphotransferase (*nptII*) gene, conferring kanamycin resistance (Table S5). The presence of cAMP-sponge transgene was also assessed by amplifying DNA of kanamycin-resistant plants with specific primers based on cAMP-sponge cDNA sequence (Table S5).

To isolate transgenic lines harbouring a single copy of the integrated gene, segregation analyses and quantitative dual target PCR (QD-PCR; Kihara *et al.*, 2006) were performed. The housekeeping single copy gene used as reference in QD-PCR was 4-hydroxyphenylpyruvate deoxygenase (*4HPPD*, At4 g03280), with the primers for *4HPPD* (Table S5). The target gene was the acquired kanamycin resistance gene (*nptII*) with the primers for *NptII* (Table S5), amplifying a 742-bp band.

Confocal microscopy analysis

Confocal laser scanning microscopy analysis of cAS-mCherry expressing seedlings (both cAS1 and cAS3 lines) was performed using a Leica SP2 confocal microscope (Leica, Germany, http://www.leica-microsystems.com). mCherry was excited at 561 nm and chlorophyll by the 488 nm line of the argon laser and the emissions were collected at 575–625 nm and 650–750 nm, respectively. Images were acquired using a HCX PL APO CS ×40/1.25 oil objective and analysed using FIJI software (http://fiji.sc/).

Determination of cAMP content

Approximately 0.1–0.15 g of *A. thaliana* leaf tissue was collected from WT and transgenic cAS plants in a 1.5-mL Eppendorf tube containing glass beads. The tubes were frozen in liquid nitrogen before mechanical grinding. Extraction buffer [25 mM Tris-HCl pH7.4, 2 mM EDTA, 2 mM PMSF, 1 mM dithiothreitol (DTT)] was added to samples, which were further homogenized mechanically. The homogenate was centrifuged (2000 ***g***, 30 min, 4°C) until complete impurity removal. The supernatant corresponding to the cytosolic fraction was further fractionated to separate free cAMP from proteins on a filter (Amicon Ultra-0.5 mL Centrifugal Filters, 10-kDa cut-off).

cAMP was further extracted from each fraction by adding ice-cold 6% TCA. The pellet was precipitated by centrifugation at 10 000 ***g*** for 5 min and repeated twice. The aqueous solution was then washed four times with 5 volumes of water-saturated diethyl ether. All these procedures were performed on ice. The samples were then frozen, lyophilized overnight and re-suspended in assay buffer without bovine serum albumin (BSA) (described below) until analysis with the Alpha-Screen cAMP assay. Anti-cAMP antibody-coated acceptor beads and streptavidin-coated donor beads were purchased from Perkin Elmer Corp. (Waltham, Massachusetts, USA). The acceptor beads and streptavidin-coated donor beads were diluted in assay buffer (25 mM HEPES, pH 7.4, 50 mM NaCl, 0.03% Tween-20) containing 1 mg mL^{-1} BSA at a concentration of 50 and 100 μg mL^{-1}, respectively. Biotinylated cAMP was re-suspended at a concentration of 1 μM in phosphate saline buffer and further mixed with the streptavidin-coated donor beads at a final concentration of 62.5 nM. The cAMP standard was prepared as a serial dilution from 0.5 nM to 5 μM in assay buffer without BSA. The reaction was carried out in white opaque 384-well plates (Optiplate TM-384, Perkin Elmer) with 10 μL of the acceptor bead mix in each well together with 5 μL of cAMP standard dilutions or samples. The plates were incubated for 30 min at room temperature in the dark before adding 10 μL of the mix containing diluted streptavidin-coated donor beads and biotinylated cAMP. The plate was incubated for further 60 min at room temperature in the dark. Fluorescence was then measured using the Enspire multilabel plate reader (Perkin Elmer).

To verify the specificity of the Alpha-Screen cAMP assay, total and free cAMP were also measured in the extracts obtained with the Amicon Ultra-0.5 mL Centrifugal Filters (10-kDa cut-off) by the cAMP-Glo™ assay kit (Promega, Madison, USA) and a microplate luminometer (Victor3 Multilabel Plate Readers, PerkinElmer, Massachusetts, USA), according to Promega's instructions (Sabetta *et al.*, 2016).

Plant infection and treatment

Pseudomonas syringae pv. *tomato* DC3000 (Pst) carrying the avirulence gene *AvrB* (*PstAvrB*) was grown overnight at 28°C in King's B medium containing the appropriate antibiotics (50 mg L^{-1} rifampicin, 50 mg L^{-1} kanamycin). Bacteria were pelleted, washed three times with 10 mM $MgCl_2$, re-suspended, and diluted in 10 mM $MgCl_2$ to the desired concentration (10^7 colony forming units (cfu) mL^{-1} corresponding to OD_{600} 0.01, unless otherwise stated). The bacterial suspension was infiltrated from the abaxial side into leaves using a 1-mL syringe without a needle. Control (mock) inoculations were carried out with 10 mM $MgCl_2$ as previously described (Hussain *et al.*, 2016; Doccula *et al.*, 2018).

Analysis of bacterial growth and HR cell death in leaves

Leaves from 6-week-old WT (Col-0) or transgenic Arabidopsis plants were infiltrated with avirulent bacterial suspensions (*PstAvrB*, 5×10^5 cfu mL^{-1}). Three days after infiltration, symptoms were observed. Analysis of bacterial growth kinetics in leaves was performed as previously described (Katagiri *et al.*, 2002) over 3 days following syringe-infiltration with avirulent bacterial suspension.

Electrolyte leakage assay was carried out to assess cell death as previously described (Imanifard *et al.*, 2018). Briefly, leaf discs were excised from leaves of 6-week-old WT or transgenic Arabidopsis plants, vacuum-infiltrated with avirulent bacterial suspension (*PstAvrB*, 1×10^7 cfu mL^{-1}), rinsed in water for 30 min and then transferred to Petri dishes containing Milli-Q water. Conductance was measured for 48 h using the B-173 compact conductivity meter (Horiba Ltd, Kyoto, Japan).

Generation of Arabidopsis cAS-mCherry plants expressing the NES-YC3.6 probe

The Arabidopsis Col-0 cAS- transgenic lines were crossed with the Col-0 pUBQ10-NES-YC3.6 line reported in Krebs *et al.* (2012). Seeds from cross-pollinated flowers were surface sterilized by vapour-

phase sterilization (Clough and Bent, 1998) and plated on MS/2 medium (MS including Vitamins, Duchefa, The Netherlands) (Murashige and Skoog, 1962) supplemented with 0.1% (w/v) sucrose, 0.05% (w/v) MES, pH 5.8 adjusted with KOH and solidified with 0.8% (w/v) of plant agar (Duchefa, The Netherlands). After stratification at 4°C in the dark for 2–3 days, seeds were transferred to the growth chamber with 16/8 h cycles of light (70 μmol photons m^{-2} sec^{-1}) at 24°C. Germinated seedlings were screened under a stereomicroscope equipped with a fluorescence lamp and scored for the simultaneous expression of both green (GFP) and red (mCherry) fluorescence. Ten-day-old positive seedlings were then transferred to pots filled with soil. Arabidopsis plants were then grown under short-day conditions (22°C, 12 h at 65 μmol photons m^{-2} sec^{-1}/18°C, 12 h dark, 70% relative humidity) in individual pots randomly distributed among standard greenhouse flats.

Ca^{2+} imaging in intact control and inoculated leaves

Whole leaves from 5- to 6-week-old cASxNES-YC3.6NES-YC3.6 plants, inoculated with 10^7 cfu mL^{-1} of avirulent *PstAvrB* or 10 mM $MgCl_2$ as a control, were cut at the level of the petiole, gently placed on a slide and covered with a coverslip (Hussain *et al.*, 2016; Doccula *et al.*, 2018), and viewed using a Nikon Ti-E inverted fluorescence microscope (Ti-E; http://www.nikon.com/) with a CFI 4× 0.13 dry objective. Excitation light was produced by a fluorescence lamp (Prior Lumen 200 PRO; Prior Scientific; http://www.prior.com) at 440 nm (436/20 nm) set to 50%. Images were collected with a Hamamatsu Dual CCD camera (ORCA-D2; http://www.hamamatsu.com/). For Cameleon analysis, the FRET CFP/YFP optical block A11400-03 (emission 1, 483/32 nm for CFP; emission 2, 542/27 nm for YFP or cpVenus) with a dichroic 510-nm mirror (Hamamatsu) was used for the simultaneous CFP and cpVenus acquisitions. Exposure time was 400 ms with a 4 × 4 CCD binning. Images where acquired every 5 sec for 1 min. Filters and the dichroic mirror were purchased from Chroma Technology (http://www.chroma.com/). NIS-Elements (Nikon; http://www.nis-elements.com/) were used as a platform to control microscope, illuminator, camera, and post-acquisition analyses. For Cameleon analysis, cpVenus and CFP emissions of the analysed regions of interest (ROIs), corresponding to the infected areas (Doccula *et al.*, 2018), were used to calculate the cpVenus/CFP ratios of individual images during the 1-min acquisition interval, and the averaged ratios were normalized to those of the mock-infiltrated plants. The experiments were repeated with three different plants and at least with two different leaves per condition per plant.

Analysis of hydrogen peroxide and redox systems

H_2O_2 was measured in WT and cAS plants according to Wang *et al.* (2014). Briefly, 0.3 g of leaves from WT and transgenic cAS line were harvested and quickly ground in liquid nitrogen and homogenized in 40 mM Tris-HCl pH 7.0 in presence of 20 μM of 2′,7′-dichlorofluorescein. The samples were incubated for 1 h in the dark and proteins were quantified using the Bradford method (Bradford, 1976). The H_2O_2 levels of the extracts (1 mg protein) were measured using a spectrofluorimeter (eccitation λ = 495 nm; emission λ = 530 nm).

Ascorbate (ASC) and glutathione (GSH) levels and redox states were measured as reported in de Pinto *et al.* (1999). Approximately 0.3 g of Arabidopsis leaf material was collected from WT and transgenic cAS lines and homogenized with 6 volumes of 5% metaphosphoric acid at 4°C. The homogenate was centrifuged at 20 000 ***g*** for 15 min at 4°C, and the supernatant used for the analysis.

For the enzymatic activities, leaves from WT and transgenic cAS line were ground in liquid nitrogen and homogenized at 4°C in 4 volumes of 50 mM Tris-HCl (pH 7.8), 0.05% (w/v) cysteine, 0.1% (w/v) BSA and 1 mM ASC. The homogenate was centrifuged at 20 000 ***g*** for 15 min at 4°C and the supernatant was analysed by spectrophotometry. Proteins were quantified using the Bradford method (Bradford, 1976) with BSA as a standard. The activities of ASC peroxidase (APX) (L-ASC:H_2O_2 oxidoreductase, EC 1.11.1.11), dehydroascorbate reductase (DHAR) (GSH: dehydroascorbate oxidoreductase, EC 1.8.5.1) and GR (NADPH:GSH disulfide oxidoreductase, EC 1.6.4.2) were determined as previously described (de Pinto *et al.*, 2000).

Quantitative real-time PCR in Arabidopsis plants

Total RNA of WT and transgenic Arabidopsis plants were isolated from young leaves using RNeasy Plant Mini Kit (Qiagen, Hilden, Germany). cDNA was synthesized from 1 μg of total RNA using the QuantiTect Reverse Transcription Kit (Qiagen) after removal of genomic DNA according to the manufacturer's instructions. RNA quality and quantity were determined using a NanoDrop 2000 spectrophotometer (Thermo Fisher Scientific).

Quantitative real-time PCR (qRT-PCR) of *cAS*, *PR1* (AT2G14610), *PDI10* (AT1G04980), *HSP90* (AT5G52640), *DJ1E* (AT2G38860), *PUB13* (AT3G46510) and *CRK14* (AT4G23220) gene expression were performed using Platinum® SYBR® Green qPCR SuperMix-UDG (Thermo Fisher Scientific). Primers used are listed in Table S6. The expression levels of these genes were calibrated by the expression of *Actin2* gene (*AT3G18780*).

TaqMan Universal PCR MasterMix (Thermo Fisher Scientific) was used for *APX-1* (AT1G07890), *APX-2* (AT3G09640), *t-APX* (AT1G77490), *s-APX* (AT4G08390) gene expression assays, using the Applied Biosystems 7900HT Fast Real-Time PCR System. Their Applied Biosystems Gene Expression Assays ID were indicated in Table S6. *GAPC2* (AT1G13440) was used as housekeeping gene. All analyses were performed on three independent plants, on three technical replicates for each sample, and reactions were repeated twice to verify the reproducibility. In all experiments, appropriate negative controls containing no template were subjected to the same procedure. The melting curve, at the end of the qPCR amplification program, was used to evaluate the formation of non-specific PCR products.

Proteomic analysis

Approximately 100 mg of leaves of Arabidopsis WT and cAS transgenic lines infected with avirulent *PstAvrB* or treated with mock were homogenized with 100 μl of extraction buffer containing 4% SDS, 5% glycerol, 40 mM Tris-HCl pH 6.8, 2× Proteinase Inhibitor Cocktail (Sigma-Aldrich). Samples were centrifuged at 21 000 ***g*** for 15 min at 4°C, supernatants were collected and then subjected to a new centrifugation. Protein content was estimated by BCA assay (Sigma-Aldrich) using BSA as standard. Two-hundred μg of protein extract were loaded on cellulose filtered columns (Microcon-30 KDa Centrifugal Filter Units, Merck), centrifuged at 10 000 ***g*** at 4°C for 5 min and subjected to the FASP protocol as published previously (Manza *et al.*, 2005). Protein digest was performed using 8 μg trypsin (Promega) in 100 mM ammonium bicarbonate and incubated overnight at 37°C in darkness with 350 rpm shaking. Peptides were collected by centrifugation at 20 870 ***g*** for 40 min. Filters were washed with 50 μl 0.5 M NaCl centrifuged at 20 870 ***g*** for 20 min to collect remaining peptides. Eluted peptides were acidified by adding 10% trifluoroacetic acid (TFA) to a final concentration of 1% TFA. Peptide mixtures were desalted using SepPak columns (Teknokroma), eluted with 60% acetonitrile (ACN) and 0.1% TFA, dried in a SpeedVac evaporator (SAVANT SPD131DDA, Thermo Fisher) and stored at −20°C

prior to mass spectrometry analysis, which was conducted as reported in Hussain *et al.* (2016).

Analysis of upstream sequences of the genes coding for the DAPs uniquely in WT plants

The upstream sequences of the genes were extracted to include only the intergenic regions (~1.5 Kb) using RSAT retrieve-seq (Nguyen *et al.*, 2018). Web-accessible bioinformatic tools to identify novel putative motifs in sets of sequences have been used, such as MEME (Bailey *et al.*, 2009) and the program 'Oligo analysis' as part of the RSAT tools (Nguyen *et al.*, 2018). MEME parameters were: the background was set to a first order Markov mode, any number of repetitions per gene, minimum width of 6 and maximum width of 12 bp. Oligo analysis parameters were as follows: the background was set to a second order Markov mode, minimum width of 6 and maximum width of 12 bp, motifs were searched on both strands. The motifs identified at least by a couple of different algorithms were used to scan the original set of sequences and to locate the putative binding sites using the program 'matrix scan' (RSAT tools). Finally, the motifs were aligned in STAMP to identify motif similarity to newly discovered and known motifs (Mahony and Benos, 2007). Motifs were searched against a collection of databases including Agris (Yilmaz *et al.*, 2011), AthaMap (Bulow *et al.*, 2009), and PLACE (Higo *et al.*, 1999). The ungapped Smith–Waterman local alignment method with a similarity score defined by Pearson's correlation coefficient estimated motif similarity.

Statistical analysis

Data are presented as mean ± standard error (SE) from three independent experiments. The statistical significance of the differences ($P < 0.05$) between groups was tested using Student's *T*-test or one-way analysis of variance (ANOVA) combined with Tukey's honestly significant difference (HSD) *post hoc* test. All the statistical analyses were performed using GraphPad Prism v4.02 software.

ACKNOWLEDGEMENTS

EV, VL, AC, and EB were supported by the Future in Research Program (FIRB 2010 – RBFR10S1LJ) funded by the Italian Ministry of Education, University and Research. The authors thank Prof. M. Hofer (Boston Healthcare System, Brigham and Women's Hospital and Harvard Medical School of Massachusetts, USA) for kindly providing 'cAMP-sponge'.

CONFLICT OF INTEREST

The authors declare no conflict of interests.

AUTHOR CONTRIBUTIONS

Conceived and designed the experiments: WS, EV, VL, AC, LV, LDG, DB, EB, MCdP. Performed the experiments: WS, EV, SC, ABM, AC, LL, DB. Analyzed and interpreted the data: WS, EV, VL, AC, SC, ABM, AG, LV, LDG, DB, EB, MCdP. Contributed reagents/materials/analysis tools: VL, EV, AC, DB, EB; wrote the paper: EV, VL, AC, EB, MCdP.

SUPPORTING INFORMATION

Additional Supporting Information may be found in the online version of this article.

Figure S1. Expression of cAMP-sponge-mCherry in Arabidopsis CAS1 line.

Figure S2. Total and free cAMP content determined by cAMP-Glo™ assay in Arabidopsis WT and cAS plants.

Figure S3. Phenotype of Arabidopsis WT and cAS plants.

Figure S4. Ascorbate and glutathione redox state in Arabidopsis WT and cAS plants in control conditions (mock) and after infection with *PstAvrB*.

Table S1. List of DAPs common to WT and cAS plants 24 hpi with *PstAvrB*.

Table S2. List of DAPs modulated only in WT plants 24 hpi with *PstAvrB*.

Table S3. List of DAPs modulated only in cAS plants 24 hpi with *PstAvrB*.

Table S4. List of DAPs in cAS vs WT plants 24 after infection with *PstAvrB*.

Table S5. Expression of genes coding for DAPs modulated only in WT and containing the CGCG motif in the negative dominant *sr1-4D* mutant treated with flg22 or infected with *Pst AvrRpm1* or *Pst AvrRps4* (data retrieved from the GSE92702 database).

Table S6. List of primers used for cloning, transgenic plant selection and for qRT-PCR analyses.

REFERENCES

Ali, R., Ma, W., Lemtiri-Chlieh, F., Tsaltas, D., Leng, Q., von Bodman, S. and Berkowitz, G.A. (2007) Death don't have no mercy and neither does calcium: Arabidopsis CYCLIC NUCLEOTIDE GATED CHANNEL2 and innate immunity. *Plant Cell*, **19**, 1081–1095.

Anderson, J.A., Huprikar, S.S., Kochian, L.V., Lucas, W.J. and Gaber, R.F. (1992) Functional expression of a probable *Arabidopsis thaliana* potassium channel in *Saccharomyces cerevisiae*. *Proc. Natl Acad. Sci. USA*, **89**, 3736–3740.

Andersson, M.X., Kourtchenko, O., Dangl, J.L., Mackey, D. and Ellerstrom, M. (2006) Phospholipase-dependent signalling during the AvrRpm1- and AvrRpt2-induced disease resistance responses in *Arabidopsis thaliana*. *Plant J.* **47**, 947–959.

Assmann, S.M. (1995) Cyclic AMP as a second messenger in higher-plants – status and future-prospects. *Plant Physiol.* **108**, 885–889.

Bailey, T.L., Boden, M., Buske, F.A., Frith, M., Grant, C.E., Clementi, L., Ren, J.Y., Li, W.W. and Noble, W.S. (2009) MEME SUITE: tools for motif discovery and searching. *Nucleic Acids Res.* **37**, W202–W208.

Balagué, C., Lin, B.Q., Alcon, C., Flottes, G., Malmstrom, S., Kohler, C., Neuhaus, G., Pelletier, G., Gaymard, F. and Roby, D. (2003) HLM1, an essential signaling component in the hypersensitive response, is a member of the cyclic nucleotide-gated channel ion channel family. *Plant Cell*, **15**, 365–379.

Bianchet, C., Wong, A., Quaglia, M., Alqurashi, M., Gehring, C., Ntoukakis, V. and Pasqualini, S. (2019) An *Arabidopsis thaliana* leucine-rich repeat protein harbors an adenylyl cyclase catalytic center and affects responses to pathogens. *J. Plant Physiol.* **232**, 12–22.

Bindschedler, L.V., Minibayeva, F., Gardner, S.L., Gerrish, C., Davies, D.R. and Bolwell, G.P. (2001) Early signalling events in the apoplastic oxidative burst in suspension cultured French bean cells involve cAMP and Ca^{2+}. *New Phytol.* **151**, 185–194.

Birkenbihl, R.P., Liu, S. and Somssich, I.E. (2017) Transcriptional events defining plant immune responses. *Curr. Opin. Plant Biol.* **38**, 1–9.

Bolton, M.D. (2009) Primary metabolism and plant defense-fuel for the fire. *Mol. Plant–Microbe Interact.* **22**, 487–497.

Bolwell, G.P. (1992) A role for phosphorylation in the down-regulation of phenylalanine ammonia-lyase in suspension-cultured cells of french bean. *Phytochemistry*, **31**, 4081–4086.

Bolwell, G.P. (1995) Cyclic AMP, the reluctant messenger in plants. *Trends Biochem. Sci.* **20**, 492–495.

Bolwell, G.P., Blee, K.A., Butt, V.S., Davies, D.R., Gardner, S.L., Gerrish, C., Minibayeva, F., Rowntree, E.G. and Wojtaszek, P. (1999) Recent advances in understanding the origin of the apoplastic oxidative burst in plant cells. *Free Radical Res.* **31**, S137–S145.

Bolwell, G.P., Bindschedler, L.V., Blee, K.A., Butt, V.S., Davies, D.R., Gardner, S.L., Gerrish, C. and Minibayeva, F. (2002) The apoplastic oxidative

burst in response to biotic stress in plants: a three-component system. *J. Exp. Bot.* **53**, 1367–1376.

Bose, J., Pottosin, I.I., Shabala, S.S., Palmgren, M.G. and Shabala, S. (2011) Calcium efflux systems in stress signaling and adaptation in plants. *Front. Plant Sci.* **2**, 85.

Bradford, M.M. (1976) A rapid and sensitive method for the quantitation of microgram quantities of protein utilizing the principle of protein-dye binding. *Anal. Biochem.* **72**, 248–254.

Bulow, L., Engelmann, S., Schindler, M. and Hehl, R. (2009) AthaMap, integrating transcriptional and post-transcriptional data. *Nucleic Acids Res.* **37**, D983–D986.

Caarls, L., Van der Does, D., Hickman, R., Jansen, W., Van Verk, M.C., Proietti, S., Lorenzo, O., Solano, R., Pieterse, C.M.J. and Van Wees, S.C.M. (2017) Assessing the role of ETHYLENE RESPONSE FACTOR transcriptional repressors in salicylic acid-mediated suppression of jasmonic acid-responsive genes. *Plant Cell Physiol.* **58**, 266–278.

Camejo, D., Guzman-Cedeno, A. and Moreno, A. (2016) Reactive oxygen species, essential molecules, during plant-pathogen interactions. *Plant Physiol. Biochem.* **103**, 10–23.

Chin, K., DeFalco, T.A., Moeder, W. and Yoshioka, K. (2013) The Arabidopsis cyclic nucleotide-gated ion channels AtCNGC2 and AtCNGC4 work in the same signaling pathway to regulate pathogen defense and floral transition. *Plant Physiol.* **163**, 611–624.

Clough, S.J. and Bent, A.F. (1998) Floral dip: a simplified method for Agrobacterium-mediated transformation of *Arabidopsis thaliana*. *Plant J.* **16**, 735–743.

Clough, S.J., Fengler, K.A., Yu, I.C., Lippok, B., Smith, R.K. and Bent, A.F. (2000) The Arabidopsis dnd1 "defense, no death" gene encodes a mutated cyclic nucleotide-gated ion channel. *Proc. Natl Acad. Sci. USA*, **97**, 9323–9328.

Cooke, C.J., Smith, C.J., Walton, T.J. and Newton, R.P. (1994) Evidence that cyclic AMP is involved in the hypersensitive response of Medicago sativa to a fungal elicitor. *Phytochemistry*, **35**, 889–895.

Cui, H.T., Tsuda, K. and Parker, J.E. (2015) Effector-triggered immunity: from pathogen perception to robust defense. *Annu. Rev. Plant Biol.* **66**, 487–511.

Curvetto, N., Darjania, L. and Delmastro, S. (1994) Effect of two cAMP analogues on stomatal opening in *Vicia faba*. Possible relationship with cytosolic calcium concentration. *Plant Physiol. Biochem.* **32**, 365–372.

D'Ambrosio, J.M., Couto, D., Fabro, G., Scuffi, D., Lamattina, L., Munnik, T., Andersson, M.X., Alvarez, M.E., Zipfel, C. and Laxalt, A.M. (2017) Phospholipase C2 affects MAMP-triggered immunity by modulating ROS production. *Plant Physiol.* **175**, 970–981.

Dangl, J.L., Dietrich, R.A. and Richberg, M.H. (1996) Death don't have no mercy: cell death programs in plant–microbe interactions. *Plant Cell*, **8**, 1793–1807.

Davies, D.R., Bindschedler, L.V., Strickland, T.S. and Bolwell, G.P. (2006) Production of reactive oxygen species in *Arabidopsis thaliana* cell suspension cultures in response to an elicitor from *Fusarium oxysporum*: implications for basal resistance. *J. Exp. Bot.* **57**, 1817–1827.

De Gara, L., de Pinto, M.C. and Tommasi, F. (2003) The antioxidant systems vis-a-vis reactive oxygen species during plant-pathogen interaction. *Plant Physiol. Biochem.* **41**, 863–870.

Doccula, F.G., Luoni, L., Behera, S., Bonza, M.C. and Costa, A. (2018) In vivo analysis of calcium levels and glutathione redox status in Arabidopsis epidermal leaf cells infected with the hypersensitive response-inducing bacteria *Pseudomonas syringae* pv. *tomato* AvrB (PstAvrB). *Methods Mol. Biol.* **1743**, 125–141.

Donaldson, L., Meier, S. and Gehring, C. (2016) The Arabidopsis cyclic nucleotide interactome. *Cell Commun. Signal.* **14**, 10.

Dong, X.N. (2004) NPR1, all things considered. *Curr. Opin. Plant Biol.* **7**, 547–552.

Du, L.Q., Ali, G.S., Simons, K.A., Hou, J.G., Yang, T.B., Reddy, A.S.N. and Poovaiah, B.W. (2009) Ca^{2+}/calmodulin regulates salicylic-acid-mediated plant immunity. *Nature*, **457**, 1154–U1116.

Ehsan, H., Reichheld, J.P., Roef, L., Witters, E., Lardon, F., Van Bockstaele, D., Van Montagu, M., Inze, D. and Van Onckelen, H. (1998) Effect of indomethacin on cell cycle dependent cyclic AMP fluxes in tobacco BY-2 cells. *FEBS Lett.* **422**, 165–169.

Faize, M., Burgos, L., Faize, L., Petri, C., Barba-Espin, G., Diaz-Vivancos, P., Clemente-Moreno, M.J., Alburquerque, N. and Hernandez, J.A. (2012) Modulation of tobacco bacterial disease resistance using cytosolic ascorbate peroxidase and Cu, Zn-superoxide dismutase. *Plant. Pathol.* **61**, 858–866.

Feechan, A., Kwon, E., Yun, B.W., Wang, Y.Q., Pallas, J.A. and Loake, G.J. (2005) A central role for S-nitrosothiols in plant disease resistance. *Proc. Natl Acad. Sci. USA*, **102**, 8054–8059.

Gao, F., Han, X.W., Wu, J.H., Zheng, S.Z., Shang, Z.L., Sun, D.Y., Zhou, R.G. and Li, B. (2012) A heat-activated calcium-permeable channel – Arabidopsis cyclic nucleotide-gated ion channel 6 – is involved in heat shock responses. *Plant J.* **70**, 1056–1069.

Gehring, C. (2010) Adenyl cyclases and cAMP in plant signaling – past and present. *Cell Commun. Signal.* **8**, 15.

Gehring, C. and Turek, I.S. (2017) Cyclic nucleotide monophosphates and their cyclases in plant signaling. *Front. Plant Sci.* **8**, 1704.

Gorecka, M., Alvarez-Fernandez, R., Slattery, K., McAusland, L., Davey, P.A., Karpinski, S., Lawson, T. and Mullineaux, P.M. (2014) Abscisic acid signalling determines susceptibility of bundle sheath cells to photoinhibition in high light-exposed Arabidopsis leaves. *Philos. Trans. R. Soc. B* **369**, 20130234.

Grant, M., Brown, I., Adams, S., Knight, M., Ainslie, A. and Mansfield, J. (2000) The RPM1 plant disease resistance gene facilitates a rapid and sustained increase in cytosolic calcium that is necessary for the oxidative burst and hypersensitive cell death. *Plant J.* **23**, 441–450.

Higo, K., Ugawa, Y., Iwamoto, M. and Korenaga, T. (1999) Plant cis-acting regulatory DNA elements (PLACE) database: 1999. *Nucleic Acids Res.* **27**, 297–300.

Holzmeister, C., Frohlich, A., Sarioglu, H., Bauer, N., Durner, J. and Lindermayr, C. (2011) Proteomic analysis of defense response of wild type *Arabidopsis thaliana* and plants with impaired NO-homeostasis. *Proteomics*, **11**, 1664–1683.

Hussain, J., Chen, J., Locato, V. *et al.* (2016) Constitutive cyclic GMP accumulation in *Arabidopsis thaliana* compromises systemic acquired resistance induced by an avirulent pathogen by modulating local signals. *Sci. Rep.* **6**, 36423.

Imanifard, Z., Vandelle, E. and Bellin, D. (2018) Measurement of hypersensitive cell death triggered by avirulent bacterial pathogens in Arabidopsis. *Methods Mol. Biol.* **1743**, 39–50.

Jacob, F., Kracher, B., Mine, A., Seyfferth, C., Blanvillain-Baufume, S., Parker, J.E., Tsuda, K., Schulze-Lefert, P. and Maekawa, T. (2018) A dominant-interfering *camta3* mutation compromises primary transcriptional outputs mediated by both cell surface and intracellular immune receptors in *Arabidopsis thaliana*. *New Phytol.* **217**, 1667–1680.

Jiang, J., Fan, L.W. and Wu, W.H. (2005) Evidences for involvement of endogenous cAMP in Arabidopsis defense responses to Verticillium toxins. *Cell Res.* **15**, 585–592.

Jones, J.D. and Dangl, J.L. (2006) The plant immune system. *Nature*, **444**, 323–329.

de Jong, C.F., Laxalt, A.M., Bargmann, B.O.R., de Wit, P.J.G.M., Joosten, M.H.A.J. and Munnik, T. (2004) Phosphatidic acid accumulation is an early response in the Cf-4/Avr4 interaction. *Plant J.* **39**, 1–12.

Jurkowski, G.I., Smith, R.K., Yu, I.C., Ham, J.H., Sharma, S.B., Klessig, D.F., Fengler, K.A. and Bent, A.F. (2004) Arabidopsis DND2, a second cyclic nucleotide-gated ion channel gene for which mutation causes the "defense, no death" phenotype. *Mol. Plant–Microbe Interact.* **17**, 511–520.

Karimi, M., Inze, D. and Depicker, A. (2002) GATEWAY((TM)) vectors for Agrobacterium-mediated plant transformation. *Trends Plant Sci.* **7**, 193–195.

Karpinski, S., Reynolds, H., Karpinska, B., Wingsle, G., Creissen, G. and Mullineaux, P. (1999) Systemic signaling and acclimation in response to excess excitation energy in Arabidopsis. *Science*, **284**, 654–657.

Katagiri, F. and Tsuda, K. (2010) Understanding the plant immune system. *Mol. Plant–Microbe Interact.* **23**, 1531–1536.

Katagiri, F., Thilmony, R. and He, S.Y. (2002) The *Arabidopsis thaliana-Pseudomonas syringae* interaction. *Arabidopsis Book*, **1**, e0039.

Kihara, T., Zhao, C.R., Kobayashi, Y., Takita, E., Kawazu, T. and Koyama, H. (2006) Simple identification of transgenic Arabidopsis plants carrying a single copy of the integrated gene. *Biosci. Biotechnol. Biochem.* **70**, 1780–1783.

Kovacs, I., Durner, J. and Lindermayr, C. (2015) Crosstalk between nitric oxide and glutathione is required for NONEXPRESSOR OF PATHOGENESIS-RELATED GENES 1 (NPR1)-dependent defense signaling in *Arabidopsis thaliana*. *New Phytol.* **208**, 860–872.

Krebs, M., Held, K., Binder, A., Hashimoto, K., Den Herder, G., Parniske, M., Kudla, J. and Schumacher, K. (2012) FRET-based genetically encoded sensors allow high-resolution live cell imaging of $Ca^{[2+]}$ dynamics. *Plant J.*, **69**, 181–192.

Kurosaki, F. and Nishi, A. (1993) Stimulation of calcium influx and calcium cascade by cyclic AMP in cultured carrot cells. *Arch. Biochem. Biophys.* **302**, 144–151.

Kurosaki, F., Tsurusawa, Y. and Nishi, A. (1987) Breakdown of phosphatidylinositol during the elicitation of phytoalexin production in cultured carrot cells. *Plant Physiol.* **85**, 601–604.

Kuzniak, E. and Sklodowska, M. (2004) Differential implication of glutathione, glutathione-metabolizing enzymes and ascorbate in tomato resistance to *Pseudomonas syringae*. *J. Phytopathol.* **152**, 529–536.

Lanubile, A., Bernardi, J., Marocco, A., Logrieco, A. and Paciolla, C. (2012) Differential activation of defense genes and enzymes in maize genotypes with contrasting levels of resistance to *Fusarium verticillioides*. *Environ. Exp. Bot.* **78**, 39–46.

Lecourieux, D., Raneva, R. and Pugin, A. (2006) Calcium in plant defence-signalling pathways. *New Phytol.* **171**, 249–269.

Lefkimmiatis, K., Moyer, M.P., Curci, S. and Hofer, A.M. (2009) "cAMP Sponge": a buffer for cyclic adenosine 3′,5′-monophosphate. *PLoS ONE*, **4**, e7649.

Lehmeyer, M., Kanofsky, K., Hanko, E.K., Ahrendt, S., Wehrs, M., Machens, F. and Hehl, R. (2016) Functional dissection of a strong and specific microbe-associated molecular pattern-responsive synthetic promoter. *Plant Biotech. J.* **14**, 61–71.

Leister, R.T., Ausubel, F.M. and Katagiri, F. (1996) Molecular recognition of pathogen attack occurs inside of plant cells in plant disease resistance specified by the Arabidopsis genes RPS2 and RPM1. *Proc. Natl Acad. Sci. USA*, **93**, 15497–15502.

Lenzoni, G., Liu, J.L. and Knight, M.R. (2018) Predicting plant immunity gene expression by identifying the decoding mechanism of calcium signatures. *New Phytol.* **217**, 1598–1609.

Levine, A., Pennell, R.I., Alvarez, M.E., Palmer, R. and Lamb, C. (1996) Calcium-mediated apoptosis in a plant hypersensitive disease resistance response. *Curr. Biol.* **6**, 427–437.

Locato, V., Cimini, S. and De Gara, L. (2018) ROS and redox balance as multifaceted players of cross-tolerance: epigenetic and retrograde control of gene expression. *J. Exp. Bot.* **69**, 3373–3391.

Lu, M., Zhang, Y.Y., Tang, S.K., Pan, J.B., Yu, Y.K., Han, J., Li, Y.Y., Du, X.H., Nan, Z.J. and Sun, Q.P. (2016) AtCNGC2 is involved in jasmonic acid-induced calcium mobilization. *J. Exp. Bot.* **67**, 809–819.

Ma, W. and Berkowitz, G.A. (2011) Ca^{2+} conduction by plant cyclic nucleotide gated channels and associated signaling components in pathogen defense signal transduction cascades. *New Phytol.* **190**, 566–572.

Ma, W., Smigel, A., Verma, R. and Berkowitz, G.A. (2009) Cyclic nucleotide gated channels and related signaling components in plant innate immunity. *Plant Signal. Behav.* **4**, 277–282.

Ma, W., Yoshioka, K., Gehring, C. and Berkowitz, G.A. (2010). The function of cyclic nucleotide-gated channels in biotic stress. In: *Ion Channels and Plant Stress Responses, Signaling and Communication in Plants* (Demidchik, V. and Maathuis, F., eds) Berlin Heidelberg: Springer-Verlag, pp. 159–174.

Maekawa, T., Kracher, B., Jacob, F. and Schulze-Lefert, P. (2017) Early ETI and PTI responses in *Arabidopsis thaliana* camta3-D (sr1-4d) mutant. https://www.ncbi.nlm.nih.gov/geo/query/acc.cgi?acc=GSE92702.

Mahony, S. and Benos, P.V. (2007) STAMP: a web tool for exploring DNA-binding motif similarities. *Nucleic Acids Res.* **35**, W253–W258.

Malik, S.I., Hussain, A., Yun, B.W., Spoel, S.H. and Loake, G.J. (2011) GSNOR-mediated de-nitrosylation in the plant defence response. *Plant Sci.* **181**, 540–544.

Manza, L.L., Stamer, S.L., Ham, A.J.L., Codreanu, S.G. and Liebler, D.C. (2005) Sample preparation and digestion for proteomic analyses using spin filters. *Proteomics*, **5**, 1742–1745.

Mou, Z., Fan, W.H. and Dong, X.N. (2003) Inducers of plant systemic acquired resistance regulate NPR1 function through redox changes. *Cell*, **113**, 935–944.

Moutinho, A., Hussey, P.J., Trewavas, A.J. and Malho, R. (2001) cAMP acts as a second messenger in pollen tube growth and reorientation. *Proc. Natl Acad. Sci. USA*, **98**, 10481–10486.

Murashige, T. and Skoog, F. (1962) A revised medium for rapid growth and bioassays with tobacco tissue cultures. *Physiol. Plant.* **15**, 473–497.

Newton, R.P. and Smith, C.J. (2004) Cyclic nucleotides. *Phytochemistry*, **65**, 2423–2437.

Nguyen, N.T.T., Contreras-Moreira, B., Castro-Mondragon, J.A. *et al.* (2018) RSAT 2018: regulatory sequence analysis tools 20th anniversary. *Nucleic Acids Res.* **46**, W209–W214.

Nomura, H., Komori, T., Uemura, S. *et al.* (2012) Chloroplast-mediated activation of plant immune signalling in Arabidopsis. *Nat. Commun.* **3**, 926.

Paciolla, C., Paradiso, A. and de Pinto, M.C. (2016) Cellular redox homeostasis as central modulator in plant stress response. In *Redox State as a Central Regulator of Plant-Cell Stress Responses* (Gupta, D.K., Palma, J.M. and Corpas, F.J., eds). Switzerland: Springer International Publishing, pp. 1–23.

Parisy, V., Poinssot, B., Owsianowski, L., Buchala, A., Glazebrook, J. and Mauch, F. (2007) Identification of PAD2 as a gamma-glutamylcysteine synthetase highlights the importance of glutathione in disease resistance of Arabidopsis. *Plant J.* **49**, 159–172.

Pietrowska-Borek, M. and Nuc, K. (2013) Both cyclic-AMP and cyclic-GMP can act as regulators of the phenylpropanoid pathway in *Arabidopsis thaliana* seedlings. *Plant Physiol. Biochem.* **70**, 142–149.

de Pinto, M.C., Francis, D. and De Gara, L. (1999) The redox state of the ascorbate-dehydroascorbate pair as a specific sensor of cell division in tobacco BY-2 cells. *Protoplasma*, **209**, 90–97.

de Pinto, M.C., Tommasi, F. and De Gara, L. (2000) Enzymes of the ascorbate biosynthesis and ascorbate-glutathione cycle in cultured cells of tobacco Bright Yellow 2. *Plant Physiol. Biochem.* **38**, 541–550.

de Pinto, M.C., Locato, V., Sgobba, A., Romero-Puertas, M.D., Gadaleta, C., Delledonne, M. and De Gara, L. (2013) S-Nitrosylation of ascorbate peroxidase is part of programmed cell death signaling in tobacco Bright Yellow-2 cells. *Plant Physiol.* **163**, 1766–1775.

de Pinto, M.C., Locato, V., Paradiso, A. and De Gara, L. (2015) Role of redox homeostasis in thermo-tolerance under a climate change scenario. *Ann. Bot.* **116**, 487–496.

Pokotylo, I., Kolesnikov, Y., Kravets, V., Zachowski, A. and Ruelland, E. (2014) Plant phosphoinositide-dependent phospholipases C: variations around a canonical theme. *Biochimie*, **96**, 144–157.

Pré, M., Atallah, M., Champion, A., De Vos, M., Pieterse, C.M.J. and Memelink, J. (2008) The AP2/ERF domain transcription factor ORA59 integrates jasmonic acid and ethylene signals in plant defense. *Plant Physiol.* **147**, 1347–1357.

Rojas, C.M., Senthil-Kumar, M., Tzin, V. and Mysore, K.S. (2014) Regulation of primary plant metabolism during plant-pathogen interactions and its contribution to plant defense. *Front. Plant Sci.* **5**, 17.

Sabetta, W., Vannini, C., Sgobba, A., Marsoni, M., Paradiso, A., Ortolani, F., Bracale, M., Viggiano, L., Blanco, E. and de Pinto, M.C. (2016) Cyclic AMP deficiency negatively affects cell growth and enhances stress-related responses in tobacco Bright Yellow-2 cells. *Plant Mol. Biol.* **90**, 467–483.

Sagi, M. and Fluhr, R. (2006) Production of reactive oxygen species by plant NADPH oxidases. *Plant Physiol.* **141**, 336–340.

Senda, K. and Ogawa, K. (2004) Induction of PR-1 accumulation accompanied by runaway cell death in the lsd1 mutant of Arabidopsis is dependent on glutathione levels but independent of the redox state of glutathione. *Plant Cell Physiol.* **45**, 1578–1585.

Shirasu, K. (2009) The HSP90-SGT1 chaperone complex for NLR immune sensors. *Annu. Rev. Plant Biol.* **60**, 139–164.

Tada, Y., Spoel, S.H., Pajerowska-Mukhtar, K., Mou, Z.L., Song, J.Q., Wang, C., Zuo, J.R. and Dong, X.N. (2008) Plant immunity requires conformational charges of NPR1 via S-nitrosylation and thioredoxins. *Science*, **321**, 952–956.

Thomas, L., Marondedze, C., Ederli, L., Pasqualini, S. and Gehring, C. (2013) Proteomic signatures implicate cAMP in light and temperature responses in *Arabidopsis thaliana*. *J. Proteomics.* **83**, 47–59.

Torres, M.A., Jones, J.D.G. and Dangl, J.L. (2006) Reactive oxygen species signaling in response to pathogens. *Plant Physiol.* **141**, 373–378.

Trewavas, A.J. (1997) Plant cyclic AMP comes in from the cold. *Nature*, **390**, 657–658.

Tsuda, K., Sato, M., Glazebrook, J., Cohen, J.D. and Katagiri, F. (2008) Interplay between MAMP-triggered and SA-mediated defense responses. *Plant J.* **53**, 763–775.

Van Damme, T., Blancquaert, D., Couturon, P., Van Der Straeten, D., Sandra, P. and Lynen, F. (2014) Wounding stress causes rapid increase in

concentration of the naturally occurring 2′,3′-isomers of cyclic guanosine- and cyclic adenosine monophosphate (cGMP and cAMP) in plant tissues. *Phytochemistry*, **103**, 59–66.

Wang, C.X., El-Shetehy, M., Shine, M.B., Yu, K.S., Navarre, D., Wendehenne, D., Kachroo, A. and Kachroo, P. (2014) Free radicals mediate systemic acquired resistance. *Cell Rep.* **7**, 348–355.

Wang, Y., Kang, Y., Ma, C. *et al.* (2017) CNGC2 is a Ca^{2+} influx channel that prevents accumulation of apoplastic Ca^{2+} in the leaf. *Plant Physiol.* **173**, 1342–1354.

Wei, H.R., Persson, S., Mehta, T., Srinivasasainagendra, V., Chen, L., Page, G.P., Somerville, C. and Loraine, A. (2006) Transcriptional coordination of the metabolic network in Arabidopsis. *Plant Physiol.* **142**, 762–774.

Wingate, V.P., Lawton, M.A. and Lamb, C.J. (1988) Glutathione causes a massive and selective induction of plant defense genes. *Plant Physiol.* **87**, 206–210.

Yadeta, K.A., Elmore, J.M., Creer, A.Y., Feng, B., Franco, J.Y., Rufian, J.S., He, P., Phinney, B. and Coaker, G. (2017) A cysteine-rich protein kinase associates with a membrane immune complex and the cysteine residues are required for cell death. *Plant Physiol.* **173**, 771–787.

Yang, T.B. and Poovaiah, B.W. (2002) A calmodulin-binding/CGCG box DNA-binding protein family involved in multiple signaling pathways in plants. *J. Biol. Chem.* **277**, 45049–45058.

Yilmaz, A., Mejia-Guerra, M.K., Kurz, K., Liang, X.Y., Welch, L. and Grotewold, E. (2011) AGRIS: the Arabidopsis gene regulatory information server, an update. *Nucleic Acids Res.* **39**, D1118–D1122.

Yoshioka, K., Moeder, W., Kang, H.G., Kachroo, P., Masmoudi, K., Berkowitz, G. and Klessig, D.F. (2006) The chimeric Arabidopsis CYCLIC NUCLEOTIDE-GATED ION CHANNEL11/12 activates multiple pathogen resistance responses. *Plant Cell*, **18**, 747–763.

Zhang, Y.Y., Zhu, H.Y., Zhang, Q., Li, M.Y., Yan, M., Wang, R., Wang, L.L., Welti, R., Zhang, W.H. and Wang, X.M. (2009) Phospholipase D alpha 1 and phosphatidic acid regulate NADPH oxidase activity and production of reactive oxygen species in ABA-mediated stomatal closure in Arabidopsis. *Plant Cell*, **21**, 2357–2377.

Zhang, Y.X., Xu, S.H., Ding, P.T. *et al.* (2010) Control of salicylic acid synthesis and systemic acquired resistance by two members of a plant-specific family of transcription factors. *Proc. Natl Acad. Sci. USA*, **107**, 18220–18225.

Zhang, L., Du, L. and Poovaiah, B.W. (2014) Calcium signaling and biotic defense responses in plants. *Plant Signal. Behav.* **9**, e973818.

Zhao, J., Guo, Y.Q., Fujita, K. and Sakai, K. (2004) Involvement of cAMP signaling in elicitor-induced phytoalexin accumulation in *Cupressus lusitanica* cell cultures. *New Phytol.* **161**, 723–733.

Zhou, W.B. and Freed, C.R. (2005) DJ-1 up-regulates glutathione synthesis during oxidative stress and inhibits A53T alpha-synuclein toxicity. *J. Biol. Chem.* **280**, 43150–43158.

Zou, J.J., Rodriguez-Zas, S., Aldea, M., Li, M., Zhu, J., Gonzalez, D.O., Vodkin, L.O., DeLucia, E. and Clough, S.J. (2005) Expression profiling soybean response to *Pseudomonas syringae* reveals new defense-related genes and rapid HR-specific downregulation of photosynthesis. *Mol. Plant–Microbe Interact.* **18**, 1161–1174.

Zulfugarov, I.S., Tovuu, A., Eu, Y.J. *et al.* (2014) Production of superoxide from Photosystem II in a rice (*Oryza sativa* L.) mutant lacking PsbS. *BMC Plant Biol.* **14**, 242.